Quantitative robust linear parameter varying H∞ vibration control of flexible structures for saving the control energy

Kai Zhang, Gérard Scorletti, Mohamed Ichchou, F. Mieyeville

Quantitative robust LPV H_∞ vibration control of flexible structures for saving the control energy

Kai Zhang

Laboratoire de Tribologie et Dynamique des Systèmes, Ecole Centrale de Lyon, 36 avenue Guy de Collongue, 69134 Ecully Cedex, France

Gérard Scorletti

Laboratoire Ampère, Ecole Centrale de Lyon, 36 avenue Guy de Collongue, 69134 Ecully Cedex, France

Mohamed Ichchou*

Laboratoire de Tribologie et Dynamique des Systèmes,Ecole Centrale de Lyon,36 avenue Guy de Collongue, 69134 Ecully Cedex,France

Fabien Mieyeville

Institut des Nanotechnologies de Lyon, Ecole Centrale de Lyon, 36 avenue Guy de Collongue, 69134 Ecully Cedex, France

Abstract

In this article, a general and systematical quantitative robust linear parameter varying (LPV) control method is proposed for active vibration control of LPV flexible structures such that a complete set of control objectives can be considered, especially, the reduction of necessarily required control energy. To achieve this goal, phase and gain control policies are employed in LPV H_∞ control designs for suitable selection of weighting functions. The

*Corresponding author
Email address: mohamed.ichchou@ec-lyon.fr (Mohamed Ichchou)

Preprint submitted to Journal of Intelligent Material Systems and StructuresJune 20, 2014

designed parameter-dependent H_∞ controller allows us to explicitly consider the time-varying parameters of the dynamical models for saving the control energy and achieving other control objectives such as the specification of vibration reduction and qualitative robustness properties to both parametric and dynamic uncertainties. Then, various reliable robustness analyses are conducted to quantitatively verify the robustness properties of the closed-loop system. The design processes and the effectiveness of the proposed control method are illustrated by active vibration control of a non-collocated piezoelectric cantilever beam excited by an external position-varying force which is the disturbance to be rejected. This plant has typical position-dependent dynamics and is modeled as an LPV system whose time-varying parameter is the actual position of the disturbance. The numerical simulations demonstrate that, compared to the classical H_∞ control and the acceleration feedback control, the proposed control method allows to compute a quantitatively robust parameter (force position) dependent controller whose benefit is to require less control energy and smaller control input, while satisfying the same control objectives in the frequency domain.

Keywords

LPV H_∞ control, phase and gain control policies, saving the control energy, parametric and dynamic uncertainties

---

1. Problem statement

Since lightweight components are widely used in practical structures for miniaturization and efficiency, these structures become more flexible and more susceptible to vibrations, which may cause significant noises, harmful

stresses, malfunctions and even failures. As a result, the flexible structures have naturally become suitable candidates for active vibration control. However, in the presence of random variations in structural properties and/or the errors in the system identification process, the obtained dynamical models inevitably have parametric uncertainties. Besides, since the flexible structures have an infinite number of resonant modes and only the first few ones can be modeled and employed in the controller designs, the high-frequency neglected dynamics are usually represented by a dynamic uncertainty, which could lead to the spillover problem [1] (Balas, 1978; Iorga et al., 2009). Considering parametria and dynamic uncertainties, in the field of robust active vibration control of flexible structures, a quantitative robust control method is proposed in Zhang et al. (2014). It employs phase-and-gain-control-policies-based output feedback H_∞ control (Zhang et al., 2013) and reliable robustness analyses to take into account a complete set of control objectives, *e.g.* the a priori determined specification of vibration reduction and the control energy are explicitly considered, and the robustness properties of the closed-loop system to parametric and dynamic uncertainties are quantitatively verified.

This control method is most suitable for Linear Time-Invariant (LTI) plants, where LTI dynamical models are used for the system modeling and an LTI H_∞ controller is correspondingly designed. Besides, all the parametric uncertainties are assumed to be within certain ranges but not measurable. However, in practice, some plants have measurable time-varying parameters,

[1] the sensor outputs are contaminated by the neglected dynamics, which we called observation spillover, and the feedback control excites the neglected dynamics, which is termed as control spillover

and thus recently Linear Parameter Varying (LPV) systems have received a rapidly increasing attention to model the dynamics of these plants, due to the fact that they can provide an interesting framework for gain-scheduling control by means of convex optimization (Rugh and Shamma, 2000; Boyd and Vandenberghe, 2004). The LPV systems constitute a class of linear systems whose dynamics usually depend on physical time-varying parameters, which are not a priori known but assumed to be measurable on-line. Such parameters are restricted to vary in predetermined sets and can be used as extra information in the control designs to synthesize parameter-dependent controllers, thus leading to improved control performances compared to classical robust control designs. The LPV system modeling and control designs have been used in a variety of applications as introduced in Mohammadpour and Scherer (2012) and the references therein.

In general, in the presence of parametric and dynamic uncertainties, there exist two approaches to the design of robust controllers for LPV systems: the controllers that do not depend on the variation of the changing parameter, but guarantee the control objectives for all possible dynamical models, *e.g.* the classical robust or the worst-case controllers as used for LTI systems; the controllers that change according to the variations of the changing parameters, *i.e.* the parameter-dependent controllers are designed. Using worst-case control designs, the dynamics of LPV systems are modeled with norm bounded uncertainties and no exact knowledge of the uncertain parameters can be considered, even it is available. In contrast, with LPV control designs, the time-varying parameters are assumed to be measured on-line and used in the LPV controller synthesis, which could provide better control performances.

It is notable that, for some particular cases as investigated in this article, both the worst-case controller and the LPV one can satisfy the specification of vibration reduction and a certain level of robustness properties. But, in addition to these normal control objectives, the designed controllers are required to consume as little control energy as possible for their practical implementations (Skogestad and Postlethwaite, 2005), since in some applications very little energy is available for active control, yet passive and semi-active methods cannot meet the control objectives, especially when the control energy is obtained from harvesting systems, *e.g.* Ichchou et al. (2011); Wang and Inman (2013a,b), and/or low-power storage devices (batteries or super capacitors) as often desirable in aerospace systems, *e.g.* Moreira et al. (2001); Yang and Sun (2002). As a result, if the control energy is not well considered or even totally neglected in the control designs, the active vibration control systems may eventually be powered off of harvested energy and/or low power storage devices. Moreover, due to the hardware limitations, the control input must be restricted by a prescribed upper bound to avoid the controller saturation and exceeding the actuator operated voltage, *e.g.* Saberi et al. (2000); Materazzi and Ubertini (2012). Exceeding the upper bound could cause unexpected behavior of the closed-loop system such as actuator damages, large overshoots, loss of control effectiveness or even a dynamic instability. In addition, as claimed in Assadian (2002), usually the vibration control capability of various controllers is measured using their effects on the sensitivity transfer function in the frequency domain. This fails to provide the control designers a physical measure for comparisons, but ranking controllers based on their energy requirements or control inputs provides an supplement and

important physical measure for the controller selection.

Therefore, an important constraint in practical active vibration control designs is the required control energy and the control input. To achieve effective robust controllers, this constraint is critical and really deserves enough attention. In the following, we have an extensive review of various techniques for saving the control energy and reducing the control input:

- Kondoh et al. (1990) propose an optimization criterion for the location selection of actuators and sensors to obtain effective vibration reduction and minimize the control energy. Bardou et al. (1997) focus on physical parameter optimization of the plate and the locations of the excitation and the actuator forces to minimize the control energy. In Lee et al. (1996) and Baz and Poh (1988), to reduce the required control energy for active vibration control of flexible structures, an optimal direct velocity feedback (DVF) control and a modified independent modal space control are respectively used to determine the optimal locations of the actuators and sensors and the control gains. Kumar and Narayanan (2008) numerically reveal that, by optimal placement of collocated piezoelectric actuators and sensors, the designed linear quadratic regulator (LQR) optimal controller can achieve effective vibration reduction of the flexible beam, while requiring a smaller control input compared to DVF control. For vibration control of a thin-walled composite beam, Zorić et al. (2013) employ the fuzzy optimization strategy to determine the size and the location of piezoelectric actuators and sensors. The particle swarm optimization (PSO) based LQR controller is then designed to maximize the closed-loop damping ratios

and minimize the control input. Besides, a literature review about optimal placement of piezoelectric actuators and sensors for minimizing the control energy can be found in Gupta et al. (2010).

- Assadian (2002) computes the control energy for active vibration control of an vibratory system and investigates the effects of control methods on the control energy, where nonoptimal DVF control, classical H_∞ control and LQR control are compared. The trade-off curves of the control energy versus the closed-loop control performance are investigated. P. Van Phuoc et al. (2009) employ a genetic algorithm for the parameter optimization of a positive position feedback (PPF) controller to minimize the control energy for active vibration reduction of a flexible robot manipulator. Similarly, Chen et al. (2011) use PSO to determine the parameters of the proportional-integral-derivative (PID) controller such that the control energy for a mass-damper-spring system is minimized.

  Wang and Inman (2011) introduce a reduced energy control (REC) law by employing a saturation control to switch the control system from one state to another one, providing conventional active controllers with a limited voltage boundary. Both experimental and numerical comparisons are performed in terms of the control energy and the setting time with PPF control, PID control, nonlinear control and LQR control. The REC law is then implemented in Wang and Inman (2013a,b) to improve unmanned aerial vehicle performance in wind gusts and reduce the control energy which is limited and harvested from ambient wing vibration. In Kumar et al. (2006), for active vibration control of an in-

verted L structure, the LQR based adaptive controller achieves robust performance and requires smaller control input compared to the pole placement method. Materazzi and Ubertini (2012) employ the 'State-dependent Riccati Equation' to reduce the control input, which consists of solving online the LQR problem with adaptive weighting functions and system matrices. In Qiu (2013), nonlinear controllers are proposed for active vibration control of a piezoelectric cantilever plate, where the control gains are computed with three nonlinear functions to adapt to the measured vibration amplitudes and regulate the control input in real-time for effective vibration reduction and avoiding the control saturation.

- With classical H_∞ control, related weighting functions are used to tune the bandwidth of the H_∞ controller, thus imposing constraints on the control energy, *e.g.* the frequency-independent weighting functions are used in Zhang et al. (2001); Huo et al. (2008), and the frequency-dependent ones are used in Sivrioglu et al. (2004); Zhang et al. (2013, 2014). Based on H_∞ loop shaping designs, Reinelt (1999, 2000, 2001) investigates active control of multivariable systems with hard bounded control input to avoid the control saturation. This control method assumes the reference signal and its first derivative to be norm bounded, and focuses on the selection of weighting functions which are explicitly related to the upper bound on the control input. The selection procedure is fulfilled until the prescribed upper bound is met and indeed user iterative as performed in Forrai et al. (2001) and Forrai et al. (2003) for active vibration control of a three-storey flexible structure.

In Kumar (2012), LQR control, classical mixed sensitivity H_∞ control, H_∞ loop shaping design and μ synthesis are used for active vibration control of a flexible beam with variable boundary conditions. These controllers are compared in terms of the required control energy and the closed-loop robust performance evaluated with μ analysis (Skogestad and Postlethwaite, 2005). It shows that, for this specifical case, the H_∞ loop shaping based controller outperforms others in terms of the control energy utilization.

Above literature review proves that, for practical active vibration control designs, it is critical to consider the constraint on the control energy and the control input. It is also shown that, in most of these researches, the constraint is achieved by kinds of optimizations of the placement and sizing of the actuators and sensors, the structural parameters, and the parameters of fixed controllers such as DVF, PID and PPF. However, as claimed in Darivandi et al. (2013), these optimization methods are generally non-convex and the dynamical models of flexible structures usually have a large number of degrees of freedom. Consequently, these optimization based methods could be inaccurate or computationally impractical. Furthermore, due to physical and installation limitations, sometimes there exists little flexibility for such optimization, for instance, although non-collocated actuators and sensors are not desirable for the closed-loop robust stability, they are unavoidable due to installation restrictions and even recommendable for high degrees of observability and controllability (Bayon de Noyer and Hanagud, 1998; Kim and Oh, 2013). Besides, the measurement of all state variables required by LQR is not always practically available, and the specification of vibration reduction and

the robustness properties cannot be quantitatively investigated with DVF, PPF, LQR, PID or nonlinear controllers.

On the other hand, the H_∞ loop shaping designs do not directly consider the control energy and only enforce the constraint on the control signal with the following inequality (Reinelt, 2000):

$$\|u(s)\|_\infty \leq 2n\|T_{ud}(s)\|_\infty \|d(s)\|_\infty \tag{1}$$

where, as shown in Figure 1, $T_{ud}(s)$ is the closed-loop transfer function form the disturbance signal $d(s)$ to the control signal $u(s)$, $\|u(s)\|_\infty$ represents the maximum amplitude of $u(s)$ and n denotes the McMillan degree of $T_{ud}(s)$ (Saberi et al., 2000). This inequality shows that decreasing $\|T_{ud}(s)\|_\infty$ reduces the upper bound for the maximum control input. Therefore, the weighting functions such as $W_1(s)$ and $W_2(s)$ are used in the H_∞ loop shaping design to adjust the open-loop transfer function $L(s) = G_p(s)K(s)$ so as to reduce $\|T_{ud}(s)\|_\infty$ according the following relationship:

$$\begin{aligned} |T_{ud}(j\omega)| &= |G_d(j\omega)K(j\omega)(1 + G_p(j\omega)K(j\omega))^{-1}| \\ &\approx |G_d(j\omega)K(j\omega)|, \text{ at frequency } |L(j\omega)| = |G_p(j\omega)K(j\omega)| \ll 1 \\ &= |G_d(j\omega)W_1(j\omega)\hat{K}_\infty(j\omega)W_2(j\omega)| \end{aligned}$$

where the controller $\hat{K}_\infty(s)$ is designed based on the shaped plant dynamical model $\hat{G}_p(s) = W_2(s)G_p(s)W_1(s)$.

These formulations provide a relationship between the upper bound for the maximum control input and related weighting functions. However, in many H_∞ loop shaping designs, *e.g.* Forrai et al. (2001, 2003), the magnitudes of related weighting functions, *e.g.* $|W_1(j\omega)|$ and $|W_2(j\omega)|$, are tuned in the

whole frequency range, that is, the selection is frequency-independent. This selection is relatively simpler than the phase-and-gain-control-policies-based frequency-dependent selection (Zhang et al., 2013). But, the gain of the corresponding controller could be very small not only at high frequencies for avoiding the spillover problem and saving the control energy, but also around the controlled resonant frequencies, thus failing to have effective vibration reduction. This implies that the frequency-independent weighting functions cannot provide a good trade-off among various control objectives.

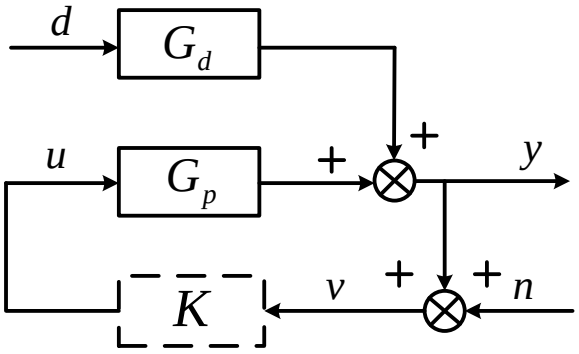

Figure 1: A typical feedback control structure for active vibration control

It is also notable that, in addition to the conservatism involved in the equality of Equation (1), the assumption that $|L(j\omega)| = |G_p(j\omega)K(j\omega)| \ll 1$ is not satisfied in the crossover regions where $|L(j\omega)| \approx 1$, and thus one cannot infer anything about $|T_{ud}(j\omega)|$ or $\|u(s)\|_\infty$ from $|L(j\omega)|$. Compared to classical H_∞ control designs, the H_∞ loop shaping designs cannot directly enforce constraints on the closed-loop transfer functions related to the set of control objectives, but just approximate these closed-loop requirements by enforcing the constraints on $|L(j\omega)|$ as some traditional control designs do. Since this approximation is not direct, there may exist considerable

errors in this approximation over certain frequency ranges. Particularly, if the control performance is explicitly defined in the frequency domain such as $|T_{yd}(j\omega)|$ for the vibration reduction, this approximation is actually not necessary. Besides, the H_∞ loop shaping designs do not explicitly consider the disturbance dynamical model $G_d(s)$, which indeed has significant effects on the set of control objectives. It is also notable that, although the LPV control techniques have been used widely, the application of LPV system modeling and associated LPV control techniques to reduce the control energy or the control input has not been specifically addressed in previous researches.

Based on above discussions, in order to tackle these critical drawbacks, the main focus of this article is placed on the application of LPV control techniques to develop a general quantitative robust active vibration control method for flexible structures such that the complete set of control objectives could be satisfied, particularly the required control energy and the control input could be reduced. In Section 2, to develop this control method, the Linear Fractional Representation (LFR) (Hecker et al., 2005; Hecker, 2006) is used to give a systematical approach for the LPV system modeling, where the scheduled variables, parametric and dynamic uncertainties can be considered uniformly. As proposed in Dinh et al. (2005), for a LTI plant considering a set of performance trade-offs parameterized by a scalar θ, several weighting functions depending on θ are incorporated into the LTI plant to develop an augmented LPV system, and an trade-off dependent H_∞ controller is synthesized by solving the finite dimensional Linear Matrix Inequality (LMI) optimization problem. In this article, an LPV plant with position-dependent dynamics has to be considered, and to save the control energy, a param-

eter (force position) dependent controller is designed thanks to the introduction of parameter-dependent weighting functions. Based on the phase and gain control policies, the weighting functions can be appropriately determined, thus developing the augmented LPV system. Then, an efficient LPV H_∞ control technique, *e.g.* Scorletti and L. EI Ghaoui (1998); Dinh et al. (2005), is used to synthesize a qualitative robust parameter-dependent H_∞ controller such that the complete set of control objectives are satisfied, especially the required control energy is reduced. To quantitatively verify the robustness properties of the closed-loop system, various robustness analyses are conducted (Zhang et al., 2014). In Section 3, the design processes and the effectiveness of the proposed control method are illustrated by active vibration control of a non-collocated piezoelectric cantilever beam, where the considered scheduled variable is the position of the external force. This is representative of the systems with parameter-dependent dynamics as investigated in Wood (1995); Paijmans et al. (2006), which could be modeled as LPV systems. In addition to the LPV H_∞ control, classical robust H_∞ control is also used for this numerical case. Their nominal control performances and the robustness properties are compared. In Section 4, the effectiveness of these controllers is compared in terms of the control energy, the control input and the system output in the time domain, which cannot be translated precisely to anything tractable in the frequency domain (Boyd and Barratt, 1992) and are not fully investigated in previous active vibration control designs (Kumar, 2012). Conclusions and perspectives are present in Section 5.

2. Proposed quantitative robust LPV control method

2.1. LPV system modeling

An LPV system is a linear system whose dynamics, *e.g.* defined by a state space representation, depend on time-varying exogenous parameters whose trajectories are a priori unknown. Nevertheless, some information is available such as the intervals to which the parameters and sometimes their derivatives belong to. More formally, let $\mathbb{R}$ denote the field of real numbers, an LPV system can be defined as following (Scorletti and Fromion, 2008b):

Definition 2.1. *LPV system*
Let the set $\Theta_t \in \mathbb{R}^{n_\theta}$ be a compact set, Θ be a set of measurable functions from $[0, \infty)$ to $\mathbb{R}^{n_\theta}$ such that for $\theta(\cdot) \in \Theta$, for all $t \geq 0$, $\theta(t) \in \Theta_t$ and

$$\begin{bmatrix} A(\theta) & B(\theta) \\ C(\theta) & D(\theta) \end{bmatrix} \tag{2}$$

be a continuous matrix function defined from $\Theta_t \in \mathbb{R}^{(n+n_o)\times(n+n_i)}$. A Linear Parameter Varying (LPV) system is defined as

$$q = \Sigma_{LPV}(p) \begin{cases} \dot{x}(t) = A(\theta(t))x(t) + B(\theta(t))p(t) \\ q(t) = C(\theta(t))x(t) + D(\theta(t))p(t) \ , \ \exists \theta(\cdot) \in \Theta \\ x(t_0) = x_0 \end{cases} \tag{3}$$

where $x(t) \in \mathbb{R}^n$ is the state vector, $p(t) \in \mathbb{R}^{n_i}$ the disturbance input, $q(t) \in \mathbb{R}^{n_o}$ the output and $\theta(t) \in \mathbb{R}^{n_\theta}$ the exogenous parameter vector assumed to be measured on-line: $\theta(t) = [\theta(t), \cdots, \theta_{n_\theta}(t)]^T$.

An LPV system is thus defined by Equation (2) and a set Θ. The LPV systems can be usually classified along the class of the set Θ and the class of

the state space matrix functions of $\Sigma_{LPV}(s,\theta)$ on θ. In this article, we focus on below class of state space matrices.

Set Θ: The compact set Θ_t is a polytope (more precisely an hyperrectangle):

$$\Theta_t = \left\{\theta = [\theta_1, \cdots, \theta_{n_\theta}]^T \mid \forall i = 1, \ldots, n_\theta\right\}$$

The set Θ is defined from Θ_t and unbounded parameter rates of variation is used (Scorletti and L. EI Ghaoui, 1998; Scherer, 2001):

$$\Theta = \{\theta(\cdot) \mid \text{for all } t \geq 0,\ \theta(t) \in \Theta_t\}$$

There are mainly two kinds of state space matrices dependence on θ: one is that the state space matrices are affine functions of θ and the other one is that the state space matrices are rational functions of θ (Scorletti and Fromion, 2008b). The later one is focused in this article, that is, any rational matrix function in Θ has an Linear Fractional Representation (LFR): there exists four matrices $A_\Sigma,\ B_\Sigma,\ C_\Sigma$ and D_Σ of compatible dimensions such that

$$\begin{bmatrix} A(\theta) & B(\theta) \\ C(\theta) & D(\theta) \end{bmatrix} = D_\Sigma + C_\Sigma \Delta_\Sigma(\theta(t))(I - A_\Sigma \Delta_\Sigma(\theta(t)))^{-1} B_\Sigma \tag{4}$$

with

$$\Delta_\Sigma(\theta(t)) = \begin{bmatrix} \theta_1(t) I_{r1} & 0 & \cdots & \cdots & 0 \\ 0 & \ddots & \ddots & & \vdots \\ \vdots & \ddots & \theta_i(t) I_{r_i} & \ddots & \vdots \\ \vdots & & \ddots & \ddots & 0 \\ 0 & \cdots & \cdots & 0 & \theta_{n_\theta}(t) I_{r_{n_\theta}} \end{bmatrix}$$

for some $r_i, i = 1, ..., n_\theta$. Such LPV systems are also referred to as Linear Fractional Transformation (LFT) systems.

2.2. Proposed LPV H_∞ control design

As performed in classical LTI H_∞ control designs, suitable weighting functions are necessary to augment the LPV plant $\Sigma_{LPV}(s,\theta)$, thus developing an augmented LPV plant $P_{au}(s,\theta)$ for the controller synthesis. As the complete set of control objectives usually have conflicting requirements on the controller, the selection of the weighting functions has to consider a trade-off among these control objectives in a rational and systematic way. Besides, in contrast with LTI H_∞ control designs, some weighting functions have to depend on θ to improve some control objectives, *e.g.* to reduce the required control energy by adapting the bandwidth of the controller to θ.

As shown in Figure 2, with the parameter-dependent input and output weighting functions, *i.e.* $W_{in}(s,\theta)$ and $W_{out}(s,\theta)$, the augmented LPV plant $P_{au}(s,\theta)$ can be developed and defined as

$$\begin{bmatrix} z \\ y \end{bmatrix} = P_{au}\left(\begin{bmatrix} w \\ u \end{bmatrix}\right) \begin{cases} \dot{x}(t) = A(\theta(t))x(t) + B_w(\theta(t))w(t) + B_u(\theta(t))u(t) \\ z(t) = C_z(\theta(t))x(t) + D_{zw}(\theta(t))w(t) + D_{zu}(\theta(t))u(t) \\ y(t) = C_y(\theta(t))x(t) + D_{yw}(\theta(t))w(t) \end{cases} \quad (5)$$

where $x(t) \in \mathbb{R}^{n_p}$ is the state vector, $u(t) \in \mathbb{R}^{n_u}$ the control input, $y(t) \in \mathbb{R}^{n_y}$ the measured output, $z(t) \in \mathbb{R}^{n_z}$ the weighted regulated output, $w(t) \in \mathbb{R}^{n_w}$ the exogenous input. The state space matrices of $P_{au}(s,\theta)$ are assumed to be rational functions of θ. Based on the definition of $P_{au}(s,\theta)$, we consider the LPV control problem:
Design an LPV controller $u = K_{LPV}(y)$ such that with the closed-loop system of Figure 2 denoted by the lower LFT $\mathcal{F}_l(P_{au}, K_{LPV})$ (Zhou et al., 1996):

- $\mathcal{F}_l(P_{au}, K_{LPV})$ is asymptotically stable;

- $\mathcal{F}_l(P_{au}, K_{LPV})$ satisfies a performance specification, for example, $\mathcal{F}_l(P_{au}, K_{LPV})$ has an $\mathcal{L}_2$ gain less than a given γ, where the $\mathcal{L}_2$ gain is defined as the smallest γ such that for any input w, $\int_0^T z(t)^T z(t)dt \leq \gamma^2 \int_0^T w(t)^T w(t)dt,\ \forall T \geq 0$. For LTI systems, the $\mathcal{L}_2$ gain is equal to the H_∞ norm. Moreover, if the $\mathcal{L}_2$ gain of $\mathcal{F}_l(P_{au}, K_{LPV})$ is no larger than γ, necessarily we have $\|\mathcal{F}_l(P_{au}(s,\theta_i), K_{LPV}(s,\theta_i))\|_\infty \leq \gamma, \forall \theta_i$.

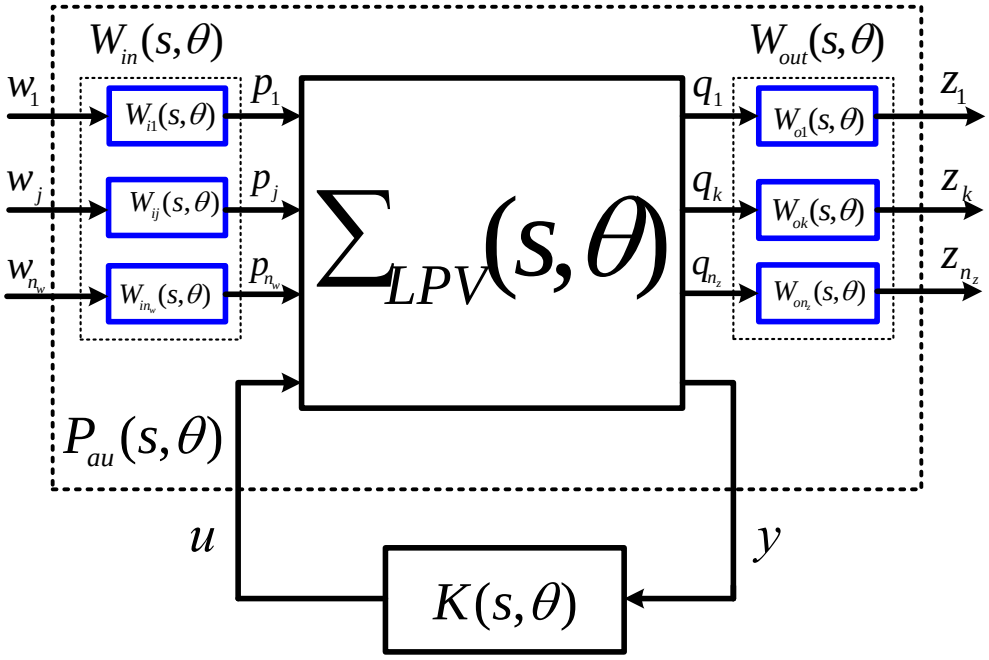

Figure 2: Augmented LPV plant $P_{au}(s,\theta)$

Evidently, the weighting functions representing the complete set of control objectives are critical to have an efficient $K_{LVP}(s,\theta)$ and have to be appropriately determined. In this article, the phase and gain control policies proposed in Zhang et al. (2013) are employed for the selection. Numerous LPV controller design approaches have been proposed since last 90's with

different levels of conservatism or computational efficiency. A classification of LPV controllers can be obtained based on the following features: the controller parameters, the feedback structure and the dependence of the state matrices of the controller on the parameters. The detailed classification of existing LPV controller, different cases of parameter dependence and available feedback structures can be found in Scorletti and Fromion (2008b). In this article, the controller state space matrices only depend on $\theta(t)$ and the output feedback control is used, that is, the output $y(t)$ of the plant $P_{au}(s,\theta)$ is assumed to be measured on-line (Scorletti and L. EI Ghaoui, 1998):

$$u = K_{LPV}(y) \begin{cases} \dot{x}_K(t) = A_K(\theta(t))x_K(t) + B_K(\theta(t))y(t) \\ \\ u(t) = C_K(\theta(t))x_K(t) + D_K(\theta(t))y(t) \end{cases} \tag{6}$$

where $x_K(t) \in \mathbb{R}^{n_K}$ and the matrices $A_K(\theta(t))$, $B_K(\theta(t))$, $C_K(\theta(t))$, $D_K(\theta(t))$ have to be synthesized. In this case, we obtain the following state space representation for the closed-loop system

$$\begin{bmatrix} A_{cl}(\theta(t)) & B_{cl}(\theta(t)) \\ C_{cl}(\theta(t)) & D_{cl}(\theta(t)) \end{bmatrix} = \begin{bmatrix} A(\theta(t)) & 0 & B_w(\theta(t)) \\ 0 & 0 & 0 \\ C_z(\theta(t)) & 0 & D_{zw}(\theta(t)) \end{bmatrix} +$$

$$\begin{bmatrix} 0 & B_u(\theta(t)) \\ I_n & 0 \\ 0 & D_{zu}(\theta(t)) \end{bmatrix} \begin{bmatrix} A_K(\theta(t)) & B_K(\theta(t)) \\ C_K(\theta(t)) & D_K(\theta(t)) \end{bmatrix} \begin{bmatrix} A_K(\theta(t)) & I_n & 0 \\ C_y(\theta(t)) & 0 & D_{yw}(\theta(t)) \end{bmatrix}$$

Considering the conservatism and computational efficiency, the LPV control technique proposed in Scorletti (1996); Scorletti and L. EI Ghaoui (1998) is employed for the LPV controller synthesis, which can be solved with LMI constraints as briefly presented in Appendix A.

With the designed LPV controller, reliable deterministic and probabilistic robustness analyses have to be conducted with μ/ν analysis and the random algorithm respectively (Zhou et al., 1996; Calafiore et al., 2000). They can take into account the probabilistic information of parametric uncertainties and quantitatively verify the robustness properties both in the deterministic sense and the probabilistic one. According to the results of the robustness analyses, if necessary, the weighting functions used in the control design can be retuned and a trade-off could be made among various control objectives. The LPV system modeling, the LPV controller design and the robustness analyses consist of the proposed quantitative robust LPV control method, which is general and allows to satisfy the complete set of control objectives. In this article, the design processes and effectiveness of the control method are subsequently illustrated with active vibration control of a piezoelectric cantilever beam excited by an external position-varying force, which has position-dependent dynamics and is modeled as an LPV system.

3. Application of the proposed control method

The proposed quantitative robust LPV control is applied to active vibration of a piezoelectric cantilever beam, as shown in Figure 3. It is excited by an external position-varying force $F(t, x_f)$, *i.e.* x_f is varying within a bounded range and assumed to be measurable in real-time. This is representative of the systems with parameter-dependent dynamics and could be modeled as an LPV system.

Based on the above discussion, some main steps are outlined for the design of a quantitative robust LPV H_∞ controller:

Step 1**:** Focus on the LPV system modeling to determine the schedule parameter θ and develop the LPV model $\Sigma_{LPV}(s,\theta)$ for the position-dependent dynamics using LFR.

Step 2**:** According to the complete set of control objectives such as the fixed specification of vibration reduction and the modulus margin, necessary weighting functions are appropriately employed based on phase and gain control policies. Especially, to fully employ the information of θ and improve some control objectives, one or several weighting functions have to depend on θ, for instance, the gain of $W_i(s,\theta)$, *i.e.* $k_{W_i}(\theta)$, depends on θ to reduce the control energy. It is critical to determine $k_{W_i}(\theta)$ in the controller design: first a finite number of allowable θ_j are chosen, which provides the corresponding LTI plant $\Sigma_{LPV}(s,\theta_j)$. Based on $\Sigma_{LPV}(s,\theta_j)$, the corresponding $k_{W_i}(\theta_j)$ and other weighting functions are selected to develop $P_{au}(s,\theta_j)$. Then one LTI H_∞ controller $K_\infty(s,\theta_j)$ is achieved to satisfy these control objectives, *e.g.* $\|\mathcal{F}_l(P_{au}(s,\theta_j),K_\infty(s,\theta_j))\|_\infty \leq 1$. Lastly, based on the chosen θ_j and the selected $k_{W_i}(\theta_j)$, the interpolation of $k_{W_i}(\theta)$ can be obtained using least mean square method to have $k_{W_i}(\theta)$ for the infinite number of allowable θ.

Step 3**:** Based on $\Sigma_{LPV}(s,\theta)$ and the weighting functions, the augmented LPV plant $P_{au}(s,\theta)$ is well developed using LFR. Then with the employed LPV control technique, the LPV controller $K_{LPV}(s,\theta)$ can be synthesized, that is, the matrices $A_K(\theta(t))$, $B_K(\theta(t))$, $C_K(\theta(t))$, $D_K(\theta(t))$ of Equation (6) are achieved.

Step 4**:** Verify that the complete set of control objectives are satisfied with the designed $K_{LPV}(s,\theta)$ for any allowable value of θ. With the weighting functions, these control objectives are reduced to $\|\mathcal{F}_l(P_{au}(s,\theta),K_{LPV}(s,\theta))\|_\infty \leq$

$1, \forall\theta$. As above discussed, when the $\mathcal{L}_2$ gain of $\mathcal{F}_l(P_{au}(s,\theta), K_{LPV}(s,\theta))$ is no larger than one, necessarily we have $\|\mathcal{F}_l(P_{au}(s,\theta), K_{LPV}(s,\theta))\|_\infty \leq 1, \forall\theta$, that is, the set of control objectives are satisfied with $K_{LPV}(s,\theta)$. Besides, in the presence of parametric and dynamic uncertainties, the robustness properties of the closed-loop system using $K_{LPV}(s,\theta)$ are quantitatively verified with deterministic and probabilistic robustness analyses. If some control objectives are not satisfied, return to Step 2 to make a better trade-off among various control objectives by adjusting the weighting functions and employ more values of θ_j for a better interpolation of $k_{W_i}(\theta)$.

3.1. LPV modeling of the position-dependent dynamics

As shown in Figure 3, the location of the accelerometer sensor and that of the piezoelectric actuator are determinant, but the location of the external force is varying within a certain range, *i.e.* x_s and x_a are fixed and the scheduled variable θ can be introduced for x_f such that

$$x_f = \theta L_{\text{beam}},\ \theta \in [\theta_{\min},\ \theta_{\max}],\ 0 < \theta_{\min} < \theta_{\max} < 1$$

where L_{beam} is the total length of the cantilever beam and $\theta_{\min}$, $\theta_{\max}$ determine the allowable position of the force.

Based on modal analysis approach (Meirovitch, 1986) and the modeling of piezoelectric actuators (Moheimani and Fleming, 2006), applying Laplace transformation and assuming zero initial conditions, for the first n resonant modes we have the formulations of the disturbance dynamical model $G_d(s)$ representing the dynamics from $F(s, x_f)$ to the beam acceleration $\ddot{Y}(x,s)$, and the plant dynamical model $G_p(s)$ representing the dynamics from the

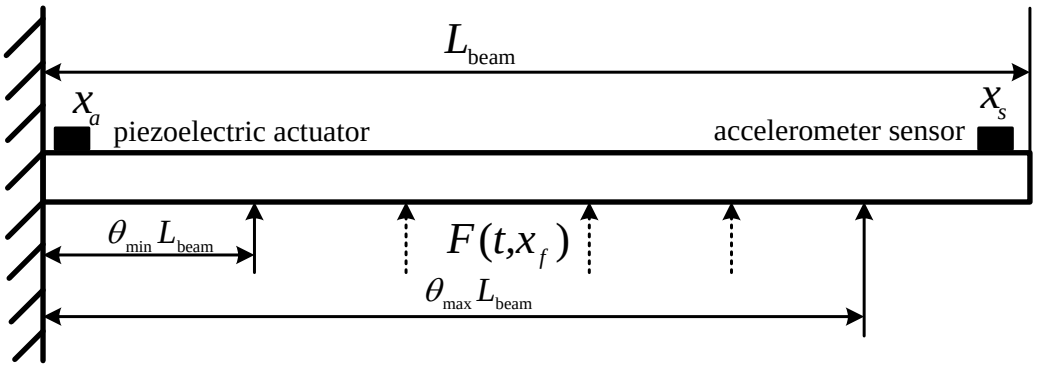

Figure 3: A piezoelectric cantilever beam with position-dependent dynamics

voltage applied on the piezoelectric actuator $V_a(x_a, s)$ to the beam acceleration $\ddot{Y}(s, x_s)$, that is,

$$G_d(s) = \frac{\ddot{Y}(s,x_s)}{F(s,x_f)} = \sum_{i=1}^{n} G_{di}(s) = \sum_{i=1}^{n} \frac{k_{di}(x_s,x_f)s^2}{s^2+2\zeta_i\omega_i+\omega_i^2}$$

$$G_p(s) = \frac{\ddot{Y}(s,x_s)}{V_a(s,x_a)} = \sum_{i=1}^{n} G_{pi}(s) = \sum_{i=1}^{n} \frac{k_{pi}(x_s,x_a)s^2}{s^2+2\zeta_i\omega_i+\omega_i^2}$$

To determine $G_d(s)$ and $G_p(s)$, we have to obtain the modal parameters such as the damping ratio ζ_i, the natural frequency ω_i and the gain $k_{pi/di}$. Based on the analytical formulations for the Euler-Bernoulli beam bounded with piezoelectric actuators (Moheimani and Fleming, 2006), ω_i and k_{pi} depend on x_s, x_a and the structural properties, *e.g.* the material properties and the geometrical dimensions. Since these elements are fixed in this case, $G_p(s)$ is determined and independent on θ. On the other hand, k_{di} depends on $x_f = \theta L_{\text{beam}}$, that is,

$$k_{di}(\theta) = g_i[\sinh(\lambda_i\theta) - \sin(\lambda_i\theta)] + h_i[\cosh(\lambda_i\theta) - \cos(\lambda_i\theta)] \qquad (7)$$

where $g_i,\ \lambda_i,\ h_i$ depend on the determinant structural properties. As shown in Figure 4, for $i = 1, 2, 3$, the gain $k_{di}(\theta)$ has particularly severe dependence on θ such that small variations in θ can generate large variations in the magnitude and the phase of $G_{di}(s)$.

Note that, for a given structure, $G_{di}(s, \theta)$ and $G_{pi}(s)$ have the same ω_i, and for the sake of simplicity, their damping ratio ζ_i is also assumed to be the same. To consider this fact and be readily employed in the control design, for the i^{th} resonant mode, it is desirable to consider the transfer function vector $[G_{di}(s, \theta),\ G_{pi}(s)]$ with the state space form:

$$A_i = \begin{bmatrix} -2\zeta_i\omega_i & 1 \\ -\omega_i^2 & 0 \end{bmatrix} \in \mathbb{R}^{2\times 2},\ B_i(\theta) = \begin{bmatrix} -2\zeta_i\omega_i \\ -\omega_i^2 \end{bmatrix} [k_{di}(\theta)\ k_{pi}] \in \mathbb{R}^{2\times 2}$$

$$C_i = \begin{bmatrix} 1 & 0 \end{bmatrix} \in \mathbb{R}^{1\times 2}, \qquad D_i(\theta) = [k_{di}(\theta)\ k_{pi}] \in \mathbb{R}^{1\times 2}$$

Naturally, when the first n resonant modes of $[G_d(s, \theta),\ G_p(s)]$ have to be

investigated, we have the state space matrices:

$$A(\theta) = \begin{bmatrix} A_1 & \mathbf{0} & \cdots & \mathbf{0} \\ \mathbf{0} & \ddots & \ddots & \vdots \\ \vdots & \ddots & \ddots & \mathbf{0} \\ \mathbf{0} & \cdots & \mathbf{0} & A_n \end{bmatrix} \in \mathbb{R}^{2n\times 2n}$$

$$B(\theta) = \begin{bmatrix} B_1(\theta) \\ \vdots \\ B_n(\theta) \end{bmatrix} = \begin{bmatrix} b_1 & \mathbf{0} & \cdots & \mathbf{0} \\ \mathbf{0} & \ddots & \ddots & \vdots \\ \vdots & \ddots & \ddots & \mathbf{0} \\ \mathbf{0} & \cdots & \mathbf{0} & b_n \end{bmatrix} \begin{bmatrix} k_d(\theta) & k_p \end{bmatrix} \in \mathbb{R}^{2n\times 2} \tag{8}$$

$$C(\theta) = \begin{bmatrix} C_1, & \cdots & , C_n \end{bmatrix} \in \mathbb{R}^{1\times 2n}$$

$$D(\theta) = [1, \cdots, 1] \begin{bmatrix} k_d(\theta), & k_p \end{bmatrix} \in \mathbb{R}^{1\times 2}$$

where $\mathbf{0}$ represents the zero matrix of a compatible dimension, $k_p = [k_{p1}, \cdots, k_{pn}]^T \in \mathbb{R}^{n\times 1}$, $k_d(\theta) = [k_{d1}(\theta), \cdots, k_{dn}(\theta)]^T \in \mathbb{R}^{n\times 1}$ and $b_i = \begin{bmatrix} -2\zeta_i\omega_i \\ -\omega_i^2 \end{bmatrix} \in \mathbb{R}^{2\times 1}$.

To appropriately consider the dependence of $k_d(\theta)$ on θ, the LFR of $k_d(\theta)$ is used:

$$k_d(\theta) = [k_{d1}(\theta), \cdots, k_{dn}(\theta)]^T = \theta\star \left[\begin{array}{c|c} A_{k_d} & B_{k_d} \\ \hline C_{k_d} & D_{k_d} \end{array}\right] \tag{9}$$

where $\star$ is the Redheffer star product (Zhou et al., 1996), the matrices $A_{k_d} \in \mathbb{R}^{m\times m}$, $B_{k_d} \in \mathbb{R}^{m\times 1}$, $C_{k_d} \in \mathbb{R}^{n\times m}$ and $D_{k_d} \in \mathbb{R}^{n\times 1}$ have to be determined, and m is the necessary fractional order for $k_d(\theta)$. Since the Equation (7) reveals that $k_{di}(\theta)$ is not a rational function of θ, in order to obtain the LFR of $k_d(\theta)$, it is necessary to approximate $k_d(\theta)$ by a rational function. For this purpose, enough samples of $\theta_j \in [\theta_{\min}, \theta_{\max}]$ are used to have the corresponding values

of $k_d(\theta_j)$, and then the least mean square method is used for the interpolation of $k_d(\theta), \theta \in [\theta_{\min}, \theta_{\max}]$. With the Equation (8) and Equation (9), we have the LFR of $[G_d(s,\theta),\ G_p(s)]$, that is,

$$[G_d(s,\theta),\ G_p(s)] = \frac{1}{s}\star \left\{ \left[\begin{array}{cccc|cccc} A_1 & \mathbf{0} & \cdots & \mathbf{0} & b_1 & \mathbf{0} & \cdots & \mathbf{0} \\ \mathbf{0} & \ddots & \ddots & \vdots & \mathbf{0} & \ddots & \ddots & \vdots \\ \vdots & \ddots & \ddots & \mathbf{0} & \vdots & \ddots & \ddots & \mathbf{0} \\ \mathbf{0} & \cdots & \mathbf{0} & A_n & \mathbf{0} & \cdots & \mathbf{0} & b_n \\ \hline C_1, & \cdots & \cdots & , C_n & 1, & \ldots & \ldots & , 1 \end{array}\right] \left[\begin{array}{c|c} I & \mathbf{0} \\ \hline \mathbf{0} & [k_d(\theta),\ k_p] \end{array}\right] \right\}$$

$$= (\frac{1}{s}, \theta)\star \left[\begin{array}{c|c} \hat{A} & \hat{B} \\ \hline \hat{C} & \hat{D} \end{array}\right] \tag{10}$$

where I represents the identity matrix of a compatible dimension, the constant matrices $\hat{A} \in \mathbb{R}^{(2n+m)\times(2n+m)}$, $\hat{B} \in \mathbb{R}^{(2n+m)\times 2}$, $\hat{C} \in \mathbb{R}^{1\times(2n+m)}$ and $\hat{D} \in \mathbb{R}^{1\times 2}$. It is notable that the vector $[k_d(\theta),\ k_p]$ in both $B(\theta)$ and $D(\theta)$ has to be pulled out to have the simplest LFR of $[G_d(s,\theta),\ G_p(s)]$ (Scorletti and Fromion, 2008a). This is desirable for the controller synthesis and the robustness analysis.

In this article, using $x_a = 3.5$mm, $x_s = 223.2$mm and the structural properties listed in Table 1, we have the nominal modal parameters for the first three resonant modes:

$$\begin{aligned} \omega_i &= [295.2, 1850.1, 5180.2], && i = 1,2,3 \\ k_{pi} &= [-8.9\times10^{-3}, 20.0\times10^{-3}, -10.4\times10^{-3}], && i = 1,2,3 \\ \zeta_i &= [20.0\times10^{-3}, 8.0\times10^{-3}, 5.0\times10^{-3}], && i = 1,2,3 \end{aligned}$$

With $\theta_{\min} = 0.4$ and $\theta_{\max} = 0.8$, the corresponding matrices for the LFR of

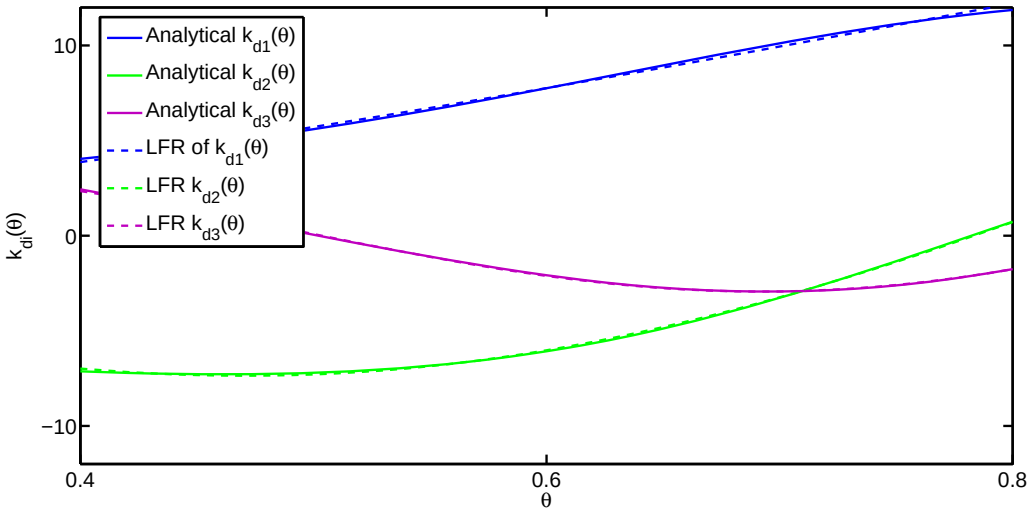

Figure 4: Analytical and LFR of $k_{di}(\theta),\ \theta \in [0.4, 0.8],\ i = [1, 2, 3]$

$k_d(\theta),\ \theta \in [0.4, 0.8]$ are

$$A_{k_d} = \begin{bmatrix} 2.10 & -1.41 \\ 1.00 & 0 \end{bmatrix},\ B_{k_d} = \begin{bmatrix} 4.00 \\ 0 \end{bmatrix}$$

$$C_{k_d} = \begin{bmatrix} 0.32 & 0.47 \\ -1.87 & 2.74 \\ -2.24 & 1.90 \end{bmatrix},\ D_{k_d} = \begin{bmatrix} 1.926 \\ -3.941 \\ 8.594 \end{bmatrix}$$

with the fractional order $m = 2$ for enough accuracy. As shown in Figure 4, this LFR of $k_d(\theta)$ has a good agreement with the analytical $k_d(\theta)$ for the first three resonant modes.

3.2. LPV and LTI H_∞ control designs

Both the proposed LPV H_∞ control design and the worst-case H_∞ control design as employed in Zhang et al. (2013) are used to achieve the same

Property	Beam	PZT	Unit
E	50.0	140.0	Gpa
l	248.0	45.0	mm
w	20.5	20.5	mm
t	4.0	1.5	mm
ρ	2500.0	/	$\mathrm{kg/m^3}$
k_{d31}	/	-1.23×10^{-10}	/

Table 1: Nominal geometrical and mechanical properties of the piezoelectric cantilever beam

fixed specification of vibration reduction defined by a frequency-dependent function $U(\omega)$. In this article, for the sake of simplicity, $U(\omega) = 40\text{dB},\ \forall\ \omega \in \mathbb{R}$, that is,

$$|T_{yd}(j\omega, \theta_j)| \leq U(\omega) = 40\text{dB},\ \forall\ \omega \in \mathbb{R},\ \forall \theta_j \in [0.4, 0.8] \tag{11}$$

where $T_{yd}(s)$ is the closed-loop transfer function from the disturbance $d(s)$ to the output $y(s)$, as shown in Figure 5.

3.2.1. LPV H_∞ control design

Based on the typical feedback control structure of Figure 1, the augmented LPV plant $P_{au}(s, \theta)$ can be well constructed by using a set of necessary and suitable weighting functions $W_i(s, \theta)$, as shown in Figure 5, where the measurement noise $n(s) = W_a(s, \theta)w_1(s)$, the disturbance $d(s) = W_b(s, \theta)w_2(s)$, the regulated signals $z_1(s) = W_1(s, \theta)v(s)$ and $z_2(s) = W_2(s, \theta)u(s)$. By partitioning $P_{au}(s, \theta)$ according to the sizes of $z(s) = [z_1(s), z_2(s)]^T$ and

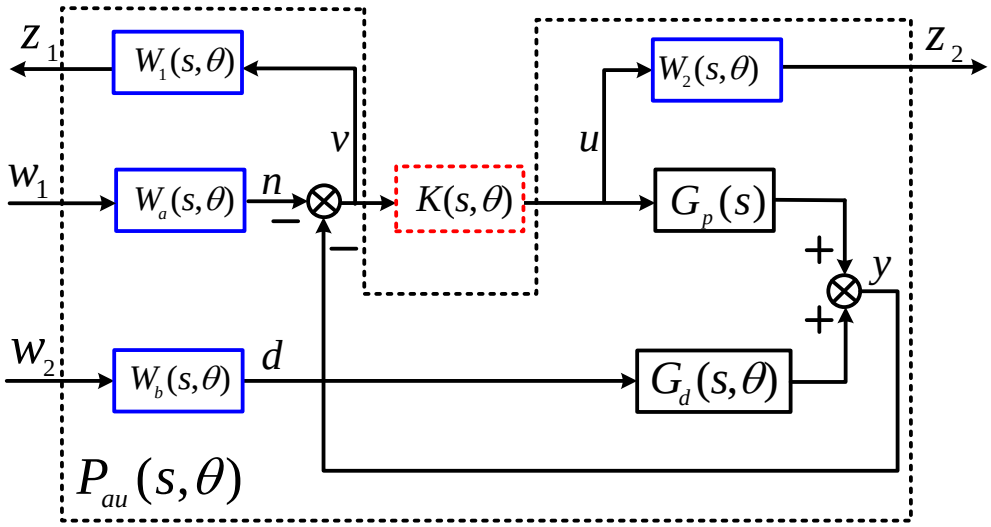

Figure 5: LPV H_∞ control structure with parameter-dependent weighting functions

$w(s) = [w_1(s), w_2(s)]^T$, $P_{au}(s,\theta)$ can be described as

$$\begin{bmatrix} z_1(s) \\ z_2(s) \\ y(s) \end{bmatrix} = P_{au}(s,\theta) \begin{bmatrix} w_1(s) \\ w_2(s) \\ u(s) \end{bmatrix}$$

To have the smallest order of $P_{au}(s,\theta)$, we have

$$P_{au}(s,\theta) = W_{\text{out}}(s,\theta) \left\{ \begin{bmatrix} 1 & 0 & 0 \\ 0 & 0 & 1 \\ -1 & 0 & 0 \end{bmatrix} + \begin{bmatrix} -1 \\ 0 \\ -1 \end{bmatrix} [G_d(s,\theta),\ G_p(s)] \begin{bmatrix} 0 & 1 & 0 \\ 0 & 0 & 1 \end{bmatrix} \right\} W_{\text{in}}(s,\theta) \tag{12}$$

with

$$W_{\text{out}}(s,\theta) = \begin{bmatrix} W_1(s,\theta) & 0 & 0 \\ 0 & W_2(s,\theta) & 0 \\ 0 & 0 & 1 \end{bmatrix} \text{ and } W_{\text{in}}(s,\theta) = \begin{bmatrix} W_a(s,\theta) & 0 & 0 \\ 0 & W_b(s,\theta) & 0 \\ 0 & 0 & 1 \end{bmatrix}$$

Substituting $[G_d(s,\theta),\ G_p(s)]$ of Equation (10) into Equation (12), we have the simplest LFR of $P_{au}(s,\theta)$, where either $[G_d(s,\theta),\ G_p(s)]$ or $W_i(s,\theta)$ occurs just one time. It is then used for the controller synthesis and the robustness analysis.

With the LPV H_∞ control design of Figure 5, $W_2(s,\theta)$ can be used to enforce constraints on the magnitudes of $|K(j\omega)S(j\omega)|$ and $|G_d(j\omega,\theta)K(j\omega)S(j\omega)|$, which are closely related to the control energy. Therefore, to adapt the control energy to θ, $W_2(s,\theta)$ has to depend on θ, and other parameter-independent weighting functions are used to determine the fixed specification of vibration reduction and the requirement on the modulus margin M_m, which is closely related to the stability robustness and defined as:

$$M_m = \inf_{\omega} |1 + L(j\omega)| = \frac{1}{\sup_{\omega} \frac{1}{|1+L(j\omega)|}} = \frac{1}{\sup_{\omega} |S(j\omega)|}, \forall \omega \in \mathbb{R} \qquad (13)$$

where $S(j\omega) = (1 + L(j\omega))^{-1}$ is the sensitivity function of the closed-loop system. Based on the Nyquist stability criterion, the larger M_m, the better stability robustness (Skogestad and Postlethwaite, 2005).

Based on the principle of phase and gain control policies, a second order $W_2(s,\theta)$ is used:

$$W_2(s,\theta) = k_{W_2}(\theta) \times \frac{(s + M\omega_b)(s + fM\omega_b)}{(s + \epsilon)(s + fM^2\omega_b)} \qquad (14)$$

where M, ω_b, ϵ, f are constants and the gain $k_{W_2}(\theta)$ determines the depen-

dance of $W_2(s,\theta)$ on θ. With LFR, $W_2(s,\theta)$ can be represented as

$$W_2(s,\theta) = \left(\frac{1}{s}\right) I_2 \star \left[\begin{array}{cc|c} 0 & 1 & 0 \\ -\epsilon f M^2 \omega_b & -(\epsilon + f M^2 \omega_b) & 1 \\ \hline (M\omega_b)^2 f - \epsilon f M^2 \omega_b & M\omega_b(1+f) - (\epsilon + f M^2 \omega_b) & 1 \end{array}\right] \times \cdots$$

$$\left[\begin{array}{cc|c} 1 & 0 & 0 \\ 0 & 1 & 0 \\ \hline 0 & 0 & k_{W_2}(\theta) \end{array}\right] \tag{15}$$

and $k_{W_2}(\theta)$ can be represented as

$$k_{W_2}(\theta) = \theta \star \left[\begin{array}{c|c} A_{k_{W_2}} & B_{k_{W_2}} \\ \hline C_{k_{W_2}} & D_{k_{W_2}} \end{array}\right] \tag{16}$$

where the parameter-independent matrices $A_{k_{W_2}} \in \mathbb{R}^{l\times l}$, $B_{k_d} \in \mathbb{R}^{l\times 1}$, $C_{k_d} \in \mathbb{R}^{1\times l}$ and $D_{k_d} \in \mathbb{R}^{1\times 1}$ have to be determined, and l is the necessary fractional order for $k_{W_2}(\theta)$. As the determination of $k_d(\theta)$, for some values of $\theta_j \in [0.4, 0.8]$, we select the corresponding value of $k_{W_2}(\theta_j)$ to satisfy the complete set of control objectives, as shown in Table 2. Then, these data can be used for the interpolation of $k_{W_2}(\theta), \forall\theta \in [0.4, 0.8]$ with the least mean square method, that is, $A_{k_{W_2}} = 4.044,\ B_{k_{W_2}} = 4.00,\ C_{k_{W_2}} = -3.637,\ D_{k_{W_2}} = -3.709$ with the fractional order $l = 1$. The other parameters of $W_2(s,\theta)$ are

θ_j	0.4	0.5	0.6	0.7	0.8
$k_{W_2}(\theta_j)$	5.4	3.7	2.4	1.8	1.5

Table 2: The chosen θ_j and $k_{W_2}(\theta_j)$ for the interpolation of $k_{W_2}(\theta)$

$M = 100.0,\ f = 35.0,\ \omega_b = 4.5,\ \epsilon = 1 \times 10^{-3}$. With these parameters, we have the LFR of $W_2(s,\theta)$ of Equation (15) and the dependence of

$|W_2(j\omega,\theta)|$ on $\theta \in [0.4, 0.8]$ is illustrated in Figure 6. In this article, to consider the fixed specification of vibration reduction of Equation (11) and ensure $M_m(\theta) \geq 0.866,\ \forall\ \omega \in \mathbb{R}$, the other constant weighting functions are $W_a(s) = 1.0,\ W_1(s) = 0.866,\ W_b(s) = 0.0115$.

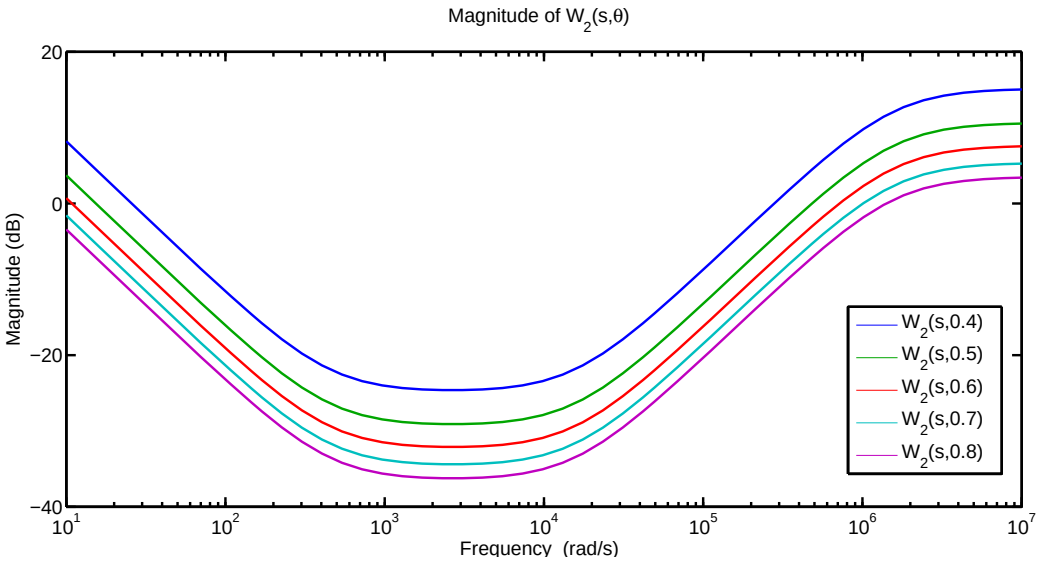

Figure 6: The dependence of $|W_2(j\omega,\theta)|$ on $\theta \in [0.4, 0.8]$

By incorporating these weighting functions into Equation (12), the simplest LFR of $P_{au}(s,\theta)$ is obtained, which is then used for the $K_{LPV}(s,\theta)$ synthesis with the LPV control technique listed in Appendix A. The LFR realization of the designed $K_{LPV}(s,\theta)$ is presented in Appendix B. With the designed $K_{LPV}(s,\theta)$, the $\mathcal{L}_2$ gain of $\mathcal{F}_l(P_{au}(s,\theta), K_{LPV}(s,\theta))$ is smaller than one, necessarily we have $\|\mathcal{F}_l(P_{au}(s,\theta_j), K_{LPV}(s,\theta_j))\|_\infty < 1$, that is, for any

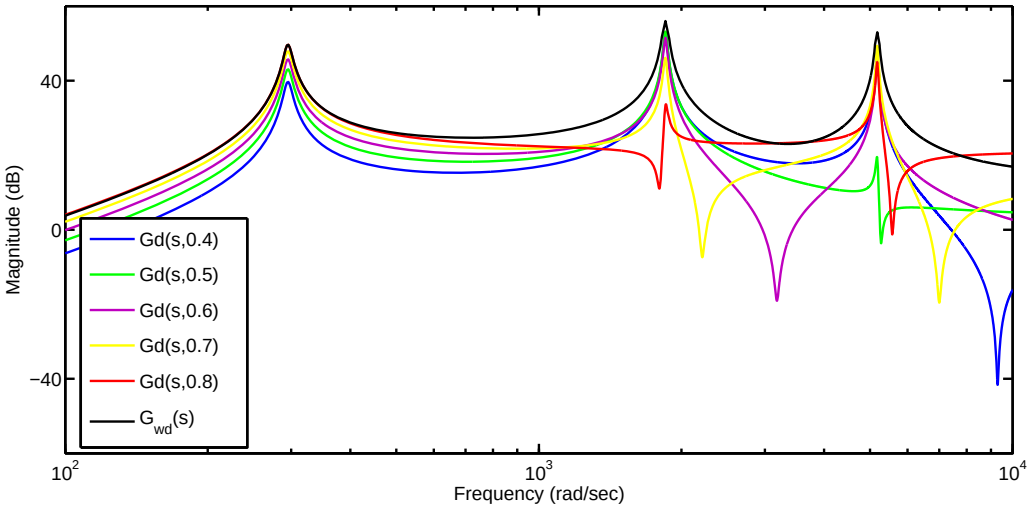

Figure 7: The worst-case $G_d(s,\theta)$ for $\theta \in [0.4, 0.8]$

$\theta_j \in [0.4, 0.8]$, we have

$$\begin{aligned} ||T_{yd}(s,\theta_j)||_\infty &< \frac{1}{\|W_1(s)W_b(s)\|_\infty} = 40\text{dB} \\ M_m(\theta_j) &= \frac{1}{\|S(s,\theta_j)\|_\infty} \geq \|W_1(s)W_a(s)\|_\infty = 0.866 \end{aligned}$$

This implies that a priori considered control objectives are simultaneously satisfied with the designed $K_{LPV}(s,\theta)$.

3.2.2. Worst-case H_∞ control design

In addition to $K_{LPV}(s,\theta)$, a worst-case H_∞ controller $K_w(s)$ is also designed in this article. First, over the frequency of interest the worst-case disturbance dynamical model $G_{wd}(s)$ is obtained by fine gridding θ of $G_d(s,\theta)$, as shown in Figure 7. Obviously, $G_{wd}(s)$ includes all possible $G_d(s,\theta)$ for any $\theta \in [0.4, 0.8]$ with very little conservatism. Then, to satisfy the same control objectives as $K_{LPV}(s,\theta)$ does, *e.g.* the specification of vibration reduction

and the requirement on M_m, the constant $W_2(s)$ is used with the parameters $M = 100.0,\ f = 35.0,\ \omega_b = 4.5,\ \epsilon = 1 \times 10^{-3},\ k_{W_2} = 2.2$. The other weighting functions are the same as used for the $K_{LPV}(s,\theta)$ synthesis. With these weighting functions, the $K_w(s)$ is obtained:

$$K_w(s) = \frac{0.1(s + 1.6 \times 10^6)(s - 255.8)(s - 1.8 \times 10^{-3})}{(s + 1.4 \times 10^4)(s + 7189.0)(s + 2050.0)} \times$$
$$\frac{(s^2 - 2801.0s + 8.6 \times 10^6)(s^2 + 9150s + 6.8 \times 10^7)}{(s^2 + 347.9s + 4.3 \times 10^4)(s^2 + 6599.0s + 4.9 \times 10^7)}$$

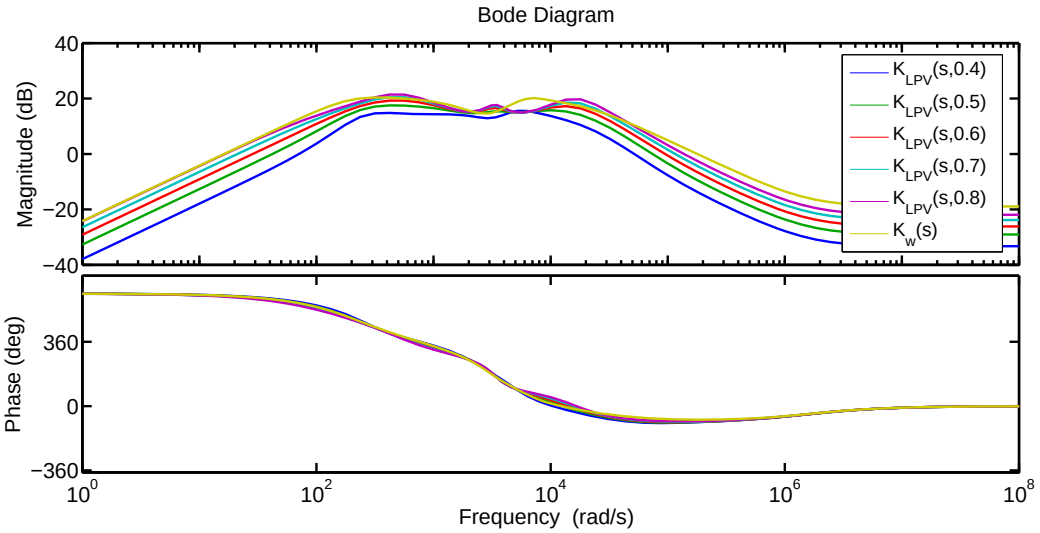

Figure 8: Comparisons between $K_{LPV}(s,\theta)$ and $K_w(s)$ for $\theta \in [0.4, 0.8]$

The comparisons between $K_{LPV}(s,\theta)$ and $K_w(s)$ in the frequency domain are illustrated in Figure 8. As expected, both $K_{LPV}(s,\theta)$ and $K_w(s)$ roll off at high frequencies to avoid the spillover problem and the $|K_{LPV}(j\omega,\theta)|$ depends on θ, which is smaller than $|K_w(j\omega)|$ at almost any frequency for $\theta \in [0.4, 0.8]$. The phases of $K_{LPV}(j\omega,\theta)$ and $K_w(j\omega)$ are nearly the same.

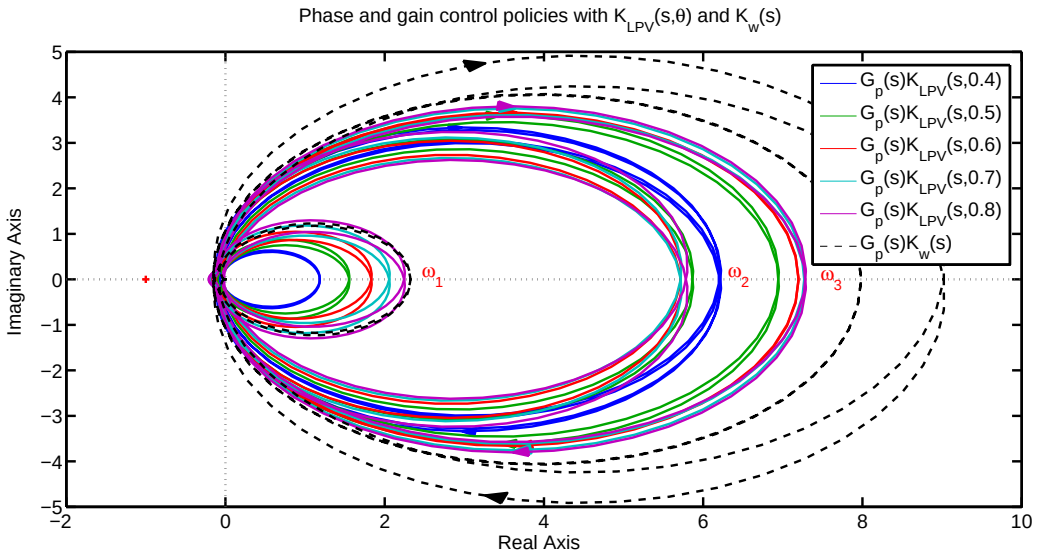

Figure 9: Phase and gain control policies with $K_{LPV}(s,\theta)$ and $K_w(s)$: ω_i represents the i^{th} controlled resonant frequency

These comparisons are consistent with the principle of phase and gain control policies. For this parameter-dependent system, the schedule variable θ only exists in $G_d(s,\theta)$ and $G_p(s)$ is independent on θ. From the phase control policy, to satisfy the fixed specification of vibration reduction while saving the control energy, $|L(j\omega,\theta) = K(s,\theta)G_p(s)|$ has to change with θ. On the other hand, for the stability robustness to parametric uncertainties, since the phase of $G_p(s)$ does not depend on θ, the phase of $K(s,\theta)$ can also be independent on θ. As illustrated in Figure 9, the Nyquist plot of $L(s,\theta_j)$ verifies that, around the controlled resonant frequencies, $|L(j\omega,\theta_j)|$ is large enough for effective vibration reduction and $L(s,\theta_j)$ stays in right half plane to have qualitative stability robustness to parametric uncertainties. The vibration reduction of the closed-loop system using $K_{LPV}(s,\theta)$ is shown in

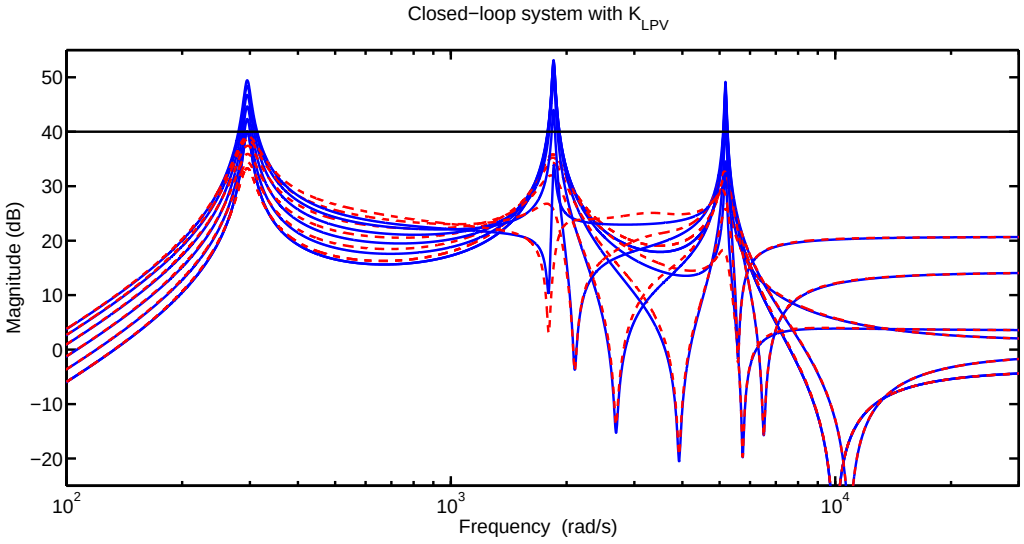

Figure 10: Closed-loop system with $K_{LPV}(s,\theta)$ for $\theta \in [0.4, 0.8]$: the blue solid curves represent the open-loop systems and the red dashed curves represent the closed-loop systems by gridded θ

Figure 10. As expected, for any allowable $\theta \in [0.4, 0.8]$, the specification of vibration reduction of Equation (11) is satisfied with $K_{LPV}(s,\theta)$. Since around the controlled resonant frequencies, $|K_{LPV}(j\omega,\theta)| < |K_w(j\omega)|, \forall\theta$, from the principle of phase control policy, $K_w(s)$ can necessarily satisfy the specification of vibration reduction.

3.3. Quantitative robustness analysis of the closed-loop system

Although, in the designs of $K_{LPV}(s,\theta)$ and $K_w(s)$, qualitative robustness properties of the closed-loop system are considered, both deterministic and probabilistic robustness analyses are necessary to quantitatively verify the robustness properties to parametric and dynamic uncertainties. In this article, the natural frequencies and damping ratios are assumed to have 20%

variations, that is,

$$\omega_i = \omega_{i0} + \omega_{i1}\delta_{\omega_i};\ |\delta_{\omega_i}| \le 1, \omega_{i1} = 0.2\omega_{i0}, i = 1,2,3$$

$$\zeta_i = \zeta_{i0} + \zeta_{i1}\delta_{\zeta_i};\ \ |\delta_{\zeta_i}| \le 1, \zeta_{i1} = 0.2\zeta_{i0},\ i = 1,2,3$$

where $\omega_{i0},\ \zeta_{i0}$ are the nominal values of these modal parameters. In addition, the scheduled variable $\theta \in [0.4, 0.8]$ is normalized such that

$$\theta = \theta_0 + \theta_1\delta_\theta;\ |\delta_\theta| \le 1$$

with $\theta_0 = 0.6$ and $\theta_1 = 0.2$. Thus, the gain $k_{di}(\theta)$ can be represented as

$$k_{di}(\theta) = k_{di0} + k_{di1}\delta_\theta;\ |\delta_\theta| \le 1, i = 1,2,3$$

where k_{di0} is obtained with $\delta_\theta = 0$. Note that, in this article, θ is assumed to be a bounded time-invariant uncertain parameter in the robustness analysis. As shown in Figure 11, the additive dynamic uncertainty $\Delta_{\rm Dyn}(s)$ is used with a suitable dynamic normalization function $W_{\rm Dyn}(s)$ to represent the neglected high-frequency dynamics of $G_p(s)$, that is,

$$G_p(s) = G_{p0}(s) + W_{\rm Dyn}(s)\Delta_{\rm Dyn}(s),\ \|\Delta_{\rm Dyn}(s)\|_\infty \le 1$$

where $G_{p0}(s)$ is the reduced nominal plant dynamical model including the first three resonant modes. To consider the robust performance, a fictitious unit-normalized performance uncertainty $\Delta_{\rm Perf}(s)$ is also used with the corresponding performance normalization function $W_{\rm Perf}(s)$ (Skogestad and Postlethwaite, 2005).

With above uncertainty modeling, the unit-normalized diagonal augmented uncertainty $\Delta' = \mathbf{diag}(\Delta'_1,\ \Delta'_2) \in \boldsymbol{B}_{\hat{\Delta}}$ can be used, where $\boldsymbol{B}_{\hat{\Delta}}$ is the

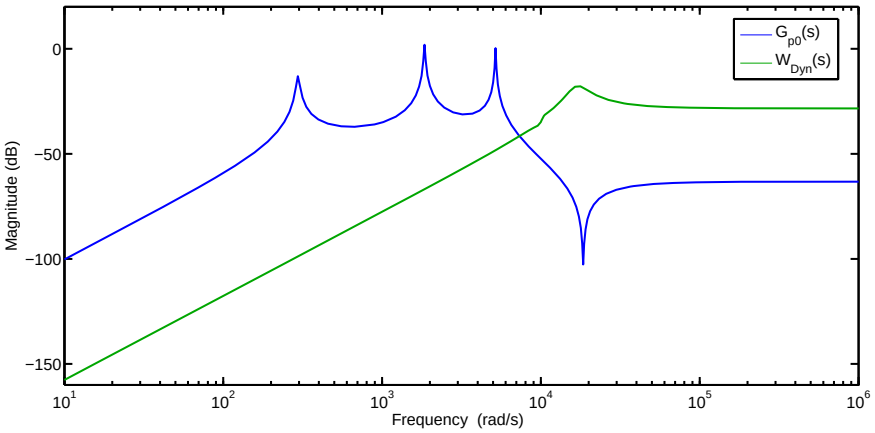

Figure 11: The additive dynamic uncertainty normalized by $W_{\mathrm{Dyn}}(s)$

norm bounded diagonal uncertainty block as defined in Zhang et al. (2014). The $\Delta_1' = \mathbf{diag}(\Delta_{\mathrm{Para}}, \Delta_{\mathrm{Dyn}})$ represents the parametric uncertainty and the dynamic one, and $\Delta_2' = \Delta_{\mathrm{Perf}}$ is the norm bounded fictitious performance uncertainty. Particularly, in this article, for the designed $K_{LPV}(s,\theta)$, we have

$$\Delta_{\mathrm{Para}} = \mathbf{diag}\ (\delta_{\omega_1} I_2, \delta_{\omega_2} I_2, \delta_{\omega_3} I_2, \delta_{\zeta_1}, \delta_{\zeta_2}, \delta_{\zeta_3}, \delta_\theta I_5)$$

where $\delta_\theta I_5$ is due to the fact that δ_θ occurs three times in $K_{LPV}(s,\theta)$ and two times in $G_d(s,\theta)$.

As performed in Zhang et al. (2014), reliable μ analysis is used to obtain the deterministic robustness margin k_{DRM} of the closed-loop system, as shown in Table 3. Since the upper and lower bounds of k_{DRM} coincide well, the estimated k_{DRM} is reliable, in other words, the closed-loop system remains stable for any $\Delta \in 1.02\Delta_1'$ with $K_w(s)$ and for any $\Delta \in 1.35\Delta_1'$ with $K_{LPV}(s,\theta)$. By ν analysis (Skogestad and Postlethwaite, 2005), we have the

deterministic worst-case performance, as illustrated in Figure 12. It shows that the specification of vibration reduction is fulfilled for any $\Delta \in 1.0\Delta_1'$ with $K_w(s)$ and $K_{LPV}(s,\theta)$. Above μ and ν analyses quantitatively ensure that the closed-loop stability and the specification of vibration reduction are satisfied in the presence of 20% variation on the modal parameters and the assumed dynamic uncertainty.

Bounds on k_{DRM}	$K_w(s)$	$K_{LPV}(s,\theta)$
Lower bound on k_{DRM}	1.355	1.020
Upper bound on k_{DRM}	1.360	1.026

Table 3: Deterministic robustness margin k_{DRM} with $K_w(s)$ and $K_{LPV}(s,\theta)$

Besides, the probabilistic robustness analysis using random algorithm is performed to consider probabilistic information of parametric uncertainties and provide complements and comparisons to the deterministic robustness analysis. For this numerical case, both uniformly and Gaussian distributed ω_i are considered and ζ_k is assumed to have uniform distribution. As performed in Zhang et al. (2014), using Monte Carlo Simulation, the results from probabilistic stability analysis are illustrated in Table 4 with $\epsilon = 0.01, \delta = 0.01$. They show that, with probability $1 - \delta = 99\%$, for either uniformly or Gaussian distributed ω_i, the closed-loop system remains stable for all sampled $\Delta \in 1.02\Delta_1'$ using $K_w(s)$ and for all sampled $\Delta \in 1.35\Delta_1'$ using $K_{LPV}(s,\theta)$. Additionally, a few destabilizing perturbations $\Delta_{\mathrm{des}} \in 1.15\Delta_1'$ are found using $K_{LPV}(s,\theta)$, which means that there exist little conservatism in the probabilistic stability analysis. These results also demonstrate that the k_{DRM} estimated from μ analysis is reliable. On the other hand, it shows that for

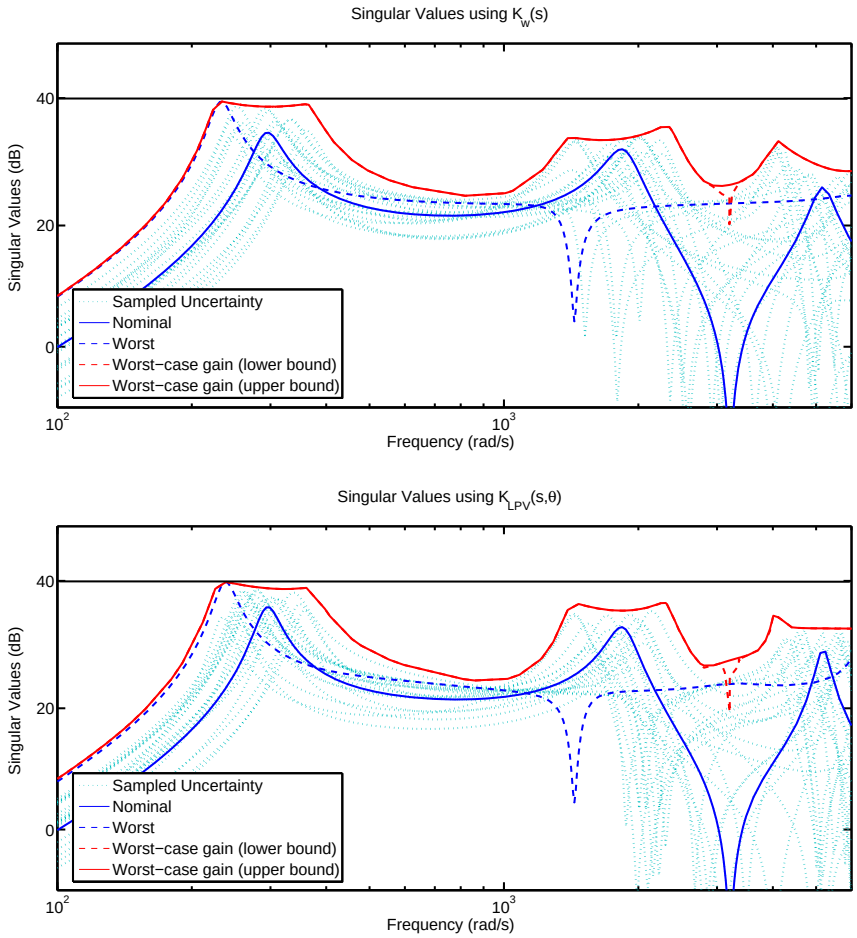

Figure 12: Deterministic worst-case performance analysis with $\Delta \in \Delta_1$

Gaussian distributed ω_i, if a 10.0% loss of probabilistic robust stability is tolerated, the corresponding $k_{\mathrm{PRM}} = 1.75$ is increased by 71.6% with respect to its deterministic counterpart $k_{\mathrm{DRM}} = 1.02$ and increased by 9.37% with respect to the result for uniformly distributed ω_i. Probabilistic worst-case performance analysis is also performed, as summarized in Table 5. It shows that, with probability 99.0%, the specification of vibration reduction is fulfilled for all sampled $\Delta_1' \in 1.00\boldsymbol{B}_{\Delta_1'}$ with $K_w(s)$ and $K_{LPV}(s,\theta)$, and when

$\Delta_1' \in 1.20\boldsymbol{B}_{\Delta_1'}$, a few perturbations can be found to violate the specification of vibration reduction. This is consistent with the result from ν analysis.

Controller	Uniformly distributed ω_i	Gaussian distributed ω_i
$K_w(s)$	$\hat{p}_n(1.35) = 100\%$	$\hat{p}_n(1.35) = 100\%$
$K_w(s)$	$\hat{p}_n(1.60) = 90\%$	$\hat{p}_n(1.65) = 90.0\%$
$K_{LPV}(s,\theta)$	$\hat{p}_n(1.02) = 100\%$	$\hat{p}_n(1.02) = 100\%$
$K_{LPV}(s,\theta)$	$\hat{p}_n(1.60) = 90\%$	$\hat{p}_n(1.75) = 90\%$

Table 4: Probabilistic stability analysis: $\epsilon = 0.01, \delta = 0.01$

Controller	Uniformly distributed ω_i	Gaussian distributed ω_i
$K_w(s)$	$\bar{\lambda}_m(1.00) = 39.75\text{dB} < 40.00\text{dB}$ $\bar{\lambda}_m(1.20) = 40.60\text{dB} > 40.00\text{dB}$	$\bar{\lambda}_m(1.00) = 39.60\text{dB} < 40.00\text{dB}$ $\bar{\lambda}_m(1.20) = 39.99\text{dB} < 40.00\text{dB}$
$K_{LPV}(s,\theta)$	$\bar{\lambda}_m(1.00) = 39.96\text{dB} < 40.00\text{dB}$ $\bar{\lambda}_m(1.20) = 45.50\text{dB} > 40.00\text{dB}$	$\bar{\lambda}_m(1.00) = 39.85\text{dB} < 40.00\text{dB}$ $\bar{\lambda}_m(1.20) = 43.94\text{dB} > 40.00\text{dB}$

Table 5: Probabilistic worst-case performance analysis: $\epsilon = 0.001, \delta = 0.01$

Above robustness analyses demonstrate that, in the presence of assumed parametric and dynamic uncertainties including the time-varying force position $\theta \in [0.4, 0.8]$, both $K_w(s)$ and $K_{LPV}(s,\theta)$ can satisfy the specification of vibration reduction and provide attractive robustness properties of the closed-loop system.

4. Performance comparisons in the time domain

As above mentioned, in this article the main motivation for the application of the proposed LPV control design is not only to design satisfying robust

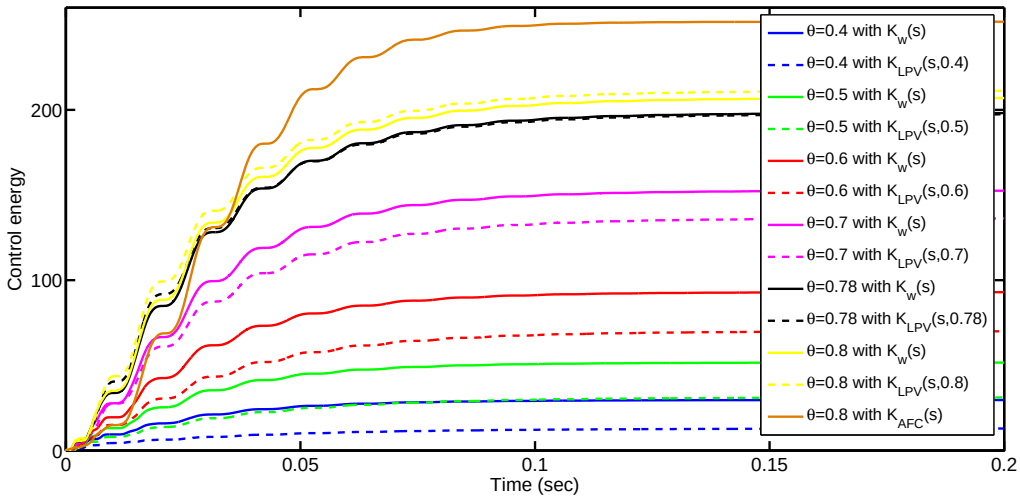

Figure 13: Comparisons of the control energy consumption using $K_w(s)$, $K_{AFC}(s)$ and $K_{LPV}(s,\theta)$

controllers for effective vibration reduction in the presence of parametric and dynamic uncertainties, but also to save the necessarily required control energy and reduce the control input. In fact, the specification of vibration reduction can be achieved with relatively simpler acceleration feedback control (AFC), for example, based on the worst-case disturbance dynamical model $G_{wd}(s)$, $K_{AFC}(s)$ can be designed for comparison purpose with the cross-over point method (Bayon de Noyer and Hanagud, 1998):

$$K_{AFC}(s) = \frac{-8.0\times 10^7(s^2+2025.0s+1.1\times 10^6)}{(s^2+165.3s+8.7\times 10^4)(s^2+1080s+3.4\times 10^6)}\times \frac{(s^2-926.1s+6.4\times 10^5)}{(s^2+2020.0s+2.7\times 10^7)}$$

As numerically verified, $K_{AFC}(s)$ can also satisfy the specification of vibration reduction as $K_w(s)$ and $K_{LPV}(s,\theta)$ do.

To emphasize the advantages of $K_{LPV}(s)$ in terms of the control energy

and the control input, within MATLAB/Simulink R2012 environment, a unit step signal is used as the external force and several numerical simulations are evaluated in the time domain. As shown in Figure 13, compared to $K_{AFC}(s)$, less control energy is required by $K_w(s)$. As explained in Zhang et al. (2013), this is mainly due to the fixed structure of AFC that makes $|K_{AFC}(j\omega)|$ too large at very low frequencies, where no control energy is actually required. Furthermore, as $G_d(s,\theta)$ depend on $\theta \in [0.4, 0.8]$, the required control energy to satisfy the fixed specification of vibration reduction greatly varies, and $K_{LPV}(s,\theta)$ has the ability to adapt its bandwidth to θ such that $K_{LPV}(s,\theta)$ consumes less control energy than $K_w(s)$ does for any $\theta \in [0.4, 0.78]$ and $K_{AFC}(s)$ does for any $\theta \in [0.4, 0.8]$. The fact that $K_{LPV}(s,\theta)$ could save the control energy is beneficial in avoiding the phenomenon of insufficient control energy and quite desirable for practical implementation, for instance, the control energy is obtained from harvesting systems or low-power storage devices (batteries or super capacitors) as often used in aerospace applications. On the other hand, as shown in Figure 14, for any $\theta \in [0.4, 0.8]$, the required control input using $K_{LPV}(s,\theta)$ is smaller than that using $K_w(s)$ or $K_{AFC}(s)$. This is useful to avoid exceeding the control saturation and the actuator operated voltage. Furthermore, $K_{LPV}(s,\theta)$, $K_w(s)$ and $K_{AFC}(s)$ can achieve not only the same specification of vibration reduction in the frequency domain and the satisfactory robustness properties as shown in Table $3-5$, but also the system output in the time domain, as illustrated in Figure 15 where the cases with $\theta = 0.4, 0.8$ are used for the sake of simplicity.

In these numerical simulations, the unit step-signal is used to simulate external disturbances. The most importance of the PSD for an unit step is at

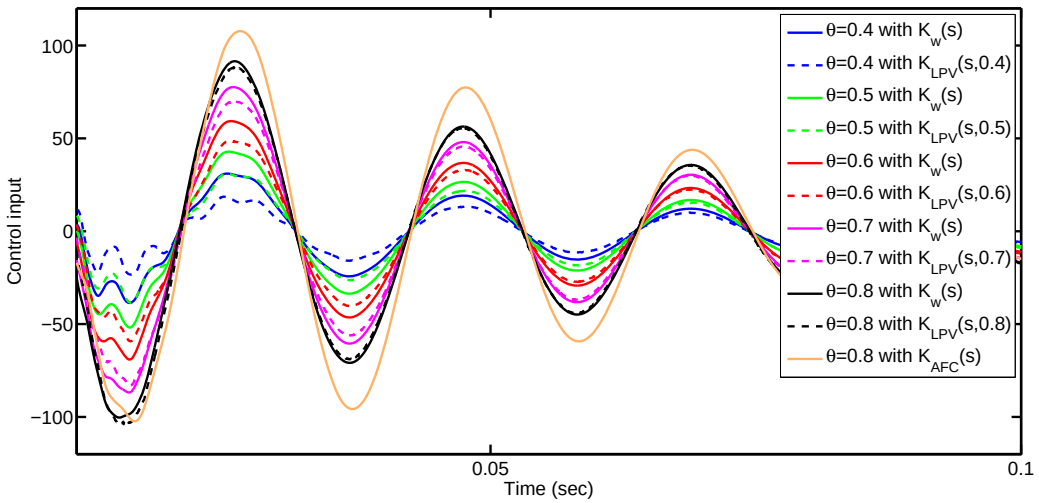

Figure 14: Comparisons of the control input using $K_w(s)$, $K_{AFC}(s)$ and $K_{LPV}(s,\theta)$

low frequencies where the considered resonant modes exist, and thus very low emphasis is focused at the high frequencies. Actually, during our simulations other signals are also used such as impulse and white noise signals which have uniform emphasis at all frequencies. With these signals, the same conclusions can be achieved, that is, compared to $K_w(s)$ and $K_{AFC}(s)$, $K_{LPV}(s,\theta)$ is particularly advantageous over the reductions of the control energy and the control input. For the sake of simplicity, the results using other signals are not specifically shown here. All of these results demonstrate that the proposed LPV H_∞ control design can provide a quantitative robust controller. Besides, considering required control energy and achieved control performances, the designed controller could be regarded to have a high cost-performance ratio.

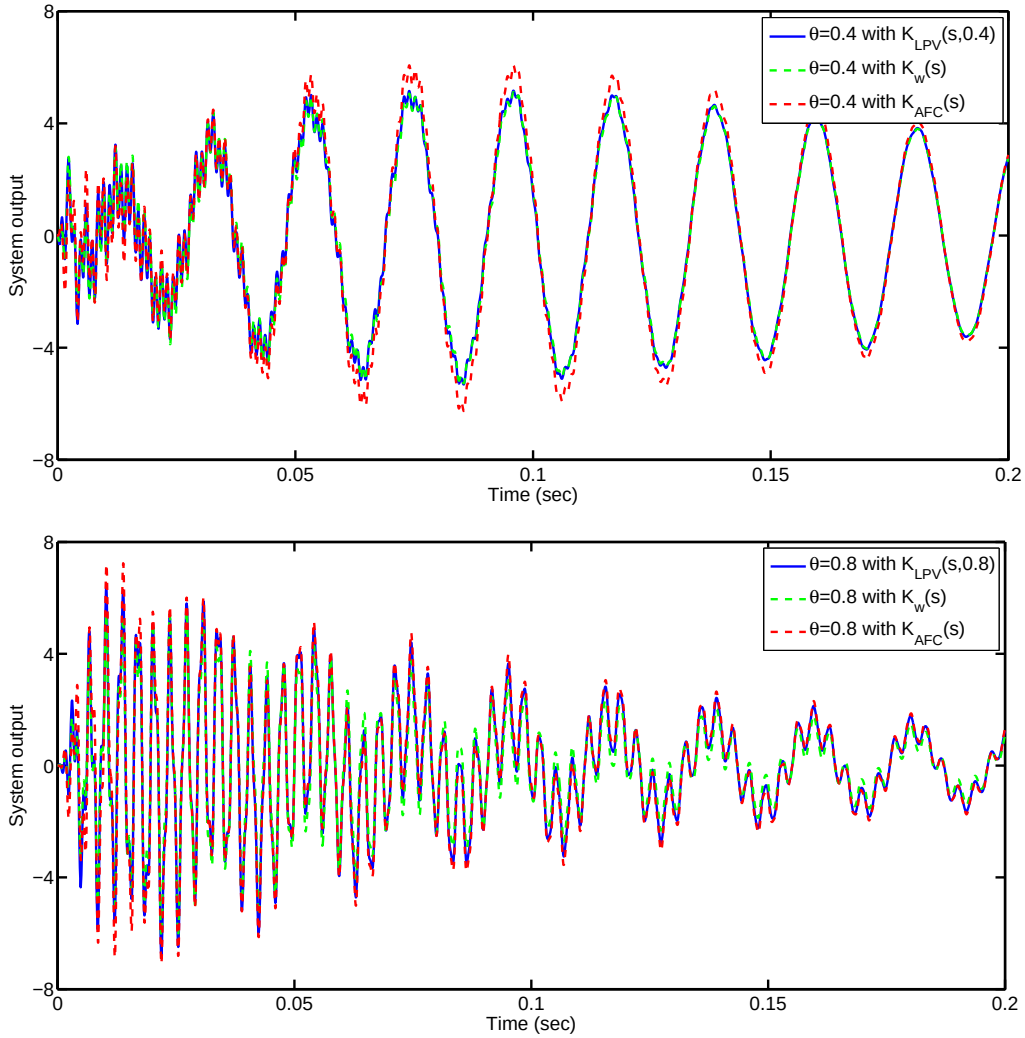

Figure 15: Comparisons of the system output using $K_w(s)$, $K_{AFC}(s)$ and $K_{LPV}(s,\theta)$ with $\theta = 0.4, 0.8$

5. Conclusions and perspectives

This research builds off of our previous researches on the quantitative robust control method for LTI systems using classical H_∞ control designs and reliable robustness analyses, and focuses on exploiting the benefits of efficient

LPV H_∞ control technique in saving the required control energy and reducing the control input. With this proposed LPV H_∞ control method, the varying parameters of the LPV system represented by θ can be fully investigated and the trade-off among various control objectives, *e.g.* the specification of vibration reduction, the closed-loop robustness properties and the saving of required control energy, can be achieved by systematical adjustments of the weighting functions which could also depend on θ. Compared to AFC and the classical H_∞ control, due to the dependence of the controller on θ, the proposed control method can explicitly save the required control energy and, in some extend, reduce the control input, while maintaining almost the same control performances both in the frequency and time domains.

In this article, some parameter-independent Lyapunov functions are used for the synthesis of $K_{LPV}(s, \theta)$. It provides a satisfactory LPV controller for the investigated case. If, in the applications under consideration, the employed parameter-independent approach appears to be very conservative, parameter dependent LMI formulations can be used for the synthesis of $K_{LPV}(s, \theta)$, which is expected to be less conservative. The details of the approach can be found in Dinh et al. (2005); Dinh (2005).

Although the motivation of this article is strongly influenced by practical application to quantitative robust active vibration control of flexible structures, it is important to appreciate that most of the design processes and employed techniques are general. In fact, many practical control problems involve the systems whose dynamics depend on some measurable exogenous parameters. For example, many vibration control systems are required to function across a variety of different temperatures, however, the variation of

ambient temperature can change the structural natural frequencies and piezoelectric stress and permittivity coefficients, thus the applied control effort has to consider such temperature dependence (Hegewald and Inman, 2001; Chettah et al., 2009; Gupta et al., 2012). This kind of control problem is readily to be handled with the proposed quantitative robust LPV H_∞ control method which considers the time-varying temperature as the scheduled variable. Furthermore, the main interest of this research is not only for active vibration control as illustrated by the studied numerical example, but rather for the fundamental issues involved in practical active control designs, for example, with few modifications, this research will be applicable to active noise control (Jemai et al., 2002), active suspensions to adapt road conditions (Fialho and Balas, 2002), active control of heating, ventilation and air condition (HVAC) systems Rasmussen and Alleyne (2010); Zhao et al. (2013), active control of machine tools N.J.M. van Dijk et al. (2010) and so on.

In addition to linear systems, LPV control methods are firstly proposed for nonlinear systems and viewed as available alternatives to classical gain-scheduling designs for controlling nonlinear systems (Carter, 1998; Rugh and Shamma, 2000). In particular, LPV control methods offer advantages over classical gain-scheduled control in that the resulting LPV controllers are automatically gain-scheduled, and no ad hoc methods of interpolation of gains are needed. Therefore, the proposed control method can also be used for active vibration control of nonlinear systems, *e.g.* Zhou et al. (2006); Ho et al. (2013).

Appendix A. Employed LPV control technique

In this article, we use the LPV control method proposed in Scorletti and L. EI Ghaoui (1998), which models the augmented LPV plant $P_{au}(s,\theta)$ with LFR and uses parameter-independent Lyapunov functions. By the scalings selection, this method allows us to make a trade-off between conservatism and computational complexity. With LFR, the $P_{au}(s,\theta)$ of Equation (5) can also be modeled as

$$\begin{bmatrix} \dot{x} \\ q \\ z \\ y \end{bmatrix} = \begin{bmatrix} M & M_u \\ M_y & 0 \end{bmatrix} \begin{bmatrix} x \\ p \\ w \\ u \end{bmatrix} \text{ and } \begin{bmatrix} x \\ p \end{bmatrix} = \Delta \begin{bmatrix} \dot{x} \\ q \end{bmatrix}$$

where $\Delta = \mathbf{diag}\left(\int I_n,\ \mathbf{diag}(\theta_i(t) I_{n_i})\right)$. Furthermore, we can assume that $\theta_{\min i} \leq \theta_i \leq \theta_{\max i}$ and thus the set Θ can be defined as

$$\Theta = \{\theta, |\theta_i \in [\theta_{\min i}, \theta_{\max i}]\} \tag{A.1}$$

This approach for obtaining a design method is the transformation of the control problem in a finite dimensional Bilinear Matrix Inequalities (BMI) optimization problem. To this end, let us introduce the following matrices

$$\mathcal{P}_M = \begin{bmatrix} I_n & 0 & 0 & 0 \\ 0 & 0 & I_n & 0 \\ 0 & I_{n_z} & 0 & 0 \\ 0 & 0 & 0 & I_{n_w} \end{bmatrix},\ \mathcal{P}_N = \begin{bmatrix} I_n & 0 & 0 & 0 \\ 0 & 0 & I_n & 0 \\ 0 & I_{n_w} & 0 & 0 \\ 0 & 0 & 0 & I_{n_z} \end{bmatrix}$$

$$\begin{aligned} X &= \mathbf{diag}(0_n, \mathbf{diag}(-2I_n)) \\ Y &= \mathbf{diag}(I_n, \mathbf{diag}((\theta_{\min i} + \theta_{\max i}) I_{n_i})) \\ Z &= \mathbf{diag}(0_n, \mathbf{diag}(-2\theta_{\min i}\theta_{\max i} I_{n_i})) \end{aligned}$$

$$\begin{bmatrix} X & Y \\ Y^T & Z \end{bmatrix} \begin{bmatrix} -\tilde{Z} & \tilde{Y}^T \\ \tilde{Y} & -\tilde{X} \end{bmatrix} = I \text{ and } \begin{bmatrix} X_{perf} & Y_{perf} \\ Y_{perf}^T & Z_{perf} \end{bmatrix} \begin{bmatrix} -\tilde{Z}_{perf} & \tilde{Y}_{perf}^T \\ \tilde{Y}_{perf} & -\tilde{X}_{perf} \end{bmatrix} = I$$

with $X_{perf} = -I,\ Y_{perf} = 0$ and $Z_{perf} = \gamma^2 I$.

Theorem Appendix A.1. *If there exist matrices S, T, G and H such that*

$$M_y^{\perp^T} \begin{bmatrix} M \\ I_{(n+n_w)} \end{bmatrix}^T \mathcal{M} \begin{bmatrix} M \\ I_{(n+n_w)} \end{bmatrix} M_y^{\perp} < 0 \tag{A.2}$$

$$M_u^{T^{\perp^T}} \begin{bmatrix} M^T \\ I_{(n+n_z)} \end{bmatrix}^T \mathcal{N} \begin{bmatrix} M^T \\ I_{(n+n_z)} \end{bmatrix} M_u^{T^{\perp}} < 0 \tag{A.3}$$

where the matrices $\mathcal{M}$ and $\mathcal{N}$ are defined as follows:

$$\mathcal{M} = \mathcal{P}_M^T \mathbf{diag}\left(\begin{bmatrix} ZS & Y^TS + G \\ YS + G^T & XS \end{bmatrix}, -\begin{bmatrix} X_{perf} & Y_{perf} \\ Y_{perf}^T & Z_{perf} \end{bmatrix} \right) \mathcal{P}_M$$

$$\mathcal{N} = \mathcal{P}_N^T \mathbf{diag}\left(\begin{bmatrix} \tilde{Z}T & \tilde{Y}^TT + H \\ \tilde{Y}T + H^T & \tilde{X}T \end{bmatrix}, -\begin{bmatrix} \tilde{X}_{perf} & \tilde{Y}_{perf} \\ \tilde{Y}_{perf}^T & \tilde{Z}_{perf} \end{bmatrix} \right) \mathcal{P}_N$$

where

$$S = \mathbf{diag}(P, \mathbf{diag}(S_i)),\quad T = \mathbf{diag}(Q, \mathbf{diag}(T_i))$$

$$G = \mathbf{diag}(0_n, \mathbf{diag}(G_i)),\ S = \mathbf{diag}(0_n, \mathbf{diag}(H_i))$$

with the $n \times n$ matrices P and Q, with the $n_i \times n_i$ matrices $S_i = S_i^T,\ T_i = T_i^T,\ G_i = -G_i^T,\ H_i = -H_i^T$ are such that

$$\begin{bmatrix} S_i & I \\ I & T_i \end{bmatrix} > 0$$

and

$$\begin{bmatrix} P & I \\ I & Q \end{bmatrix} > 0$$

then there exist an LPV controller such that the closed-loop system is internally stable with an $\mathcal{L}_2$ gain less than γ.

This theorem actually presents a set of LMI constraints: first, a given γ is used to test the conditions of the previous theorem; then, the smallest γ is searched to satisfy the conditions of the theorem. If theses conditions can be satisfied, the matrices of the LFR representation of $K_{LPV}(s,\theta)$ can be using a feasibility optimization problem. Explicit formulations of this optimization problem can be found in Scorletti and L. EI Ghaoui (1998).

Appendix B. LFR realization of the designed $\boldsymbol{K_{LPV}(s,\theta)}$

As illustrated with the Figure B.16, the input-output realization of the designed $K_{LPV}(s,\theta)$ is $y = \mathcal{F}_u(M,\Delta)u$ with $\Delta = \text{diag}(I_8/s, I_3\theta)$, where $\mathcal{F}_u$ is the upper LFT, the matrix M is defined on the page 19 of J-F. Magni (2006) and can be appropriately partitioned according to the order of the controller and the size of θ, *e.g.* 8 is equal to the order of $P_{au}(s,\theta)$ and 3 is the sum of $m = 2$ and $l = 1$.

By directly closing the θ loop of Figure B.16, the matrices defined in

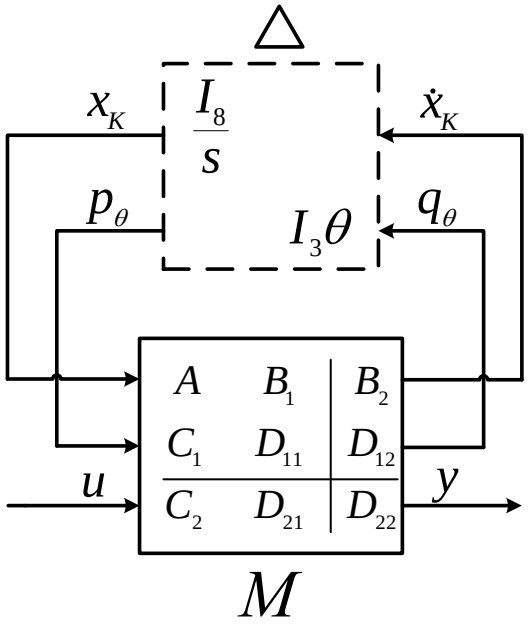

Figure B.16: LFR realization of $K_{LPV}(s,\theta)$

Equation (6) are obtained, that is,

$$\begin{aligned}
A_K(\theta(t)) &= A + B_1 I_3 \theta(t)(I - D_{11} I_3 \theta(t))^{-1} C_1 \\
B_K(\theta(t)) &= B_2 + B_1 I_3 \theta(t)(I - D_{11} I_3 \theta(t))^{-1} D_{12} \\
C_K(\theta(t)) &= C_2 + D_{21} I_3 \theta(t)(I - D_{11} I_3 \theta(t))^{-1} C_1 \\
D_K(\theta(t)) &= D_{22} + D_{21} I_3 \theta(t)(I - D_{11} I_3 \theta(t))^{-1} D_{12}
\end{aligned}$$

Note that from the lemma 3.2.1 in J-F. Magni (2006), it is known that the input-output LFR realization of $K_{LPV}(s,\theta)$, that is,

$$y = \mathcal{F}_u \left(\begin{bmatrix} A & B_1 & B_2 \\ C_1 & D_{11} & D_{12} \\ C_2 & D_{21} & D_{22} \end{bmatrix}, \begin{bmatrix} \frac{I_8}{s} & 0 \\ 0 & I_3\theta \end{bmatrix} \right) u$$

can also be realized by the equivalent state-space LFR

$$\begin{bmatrix} \dot{x}_K \\ y \end{bmatrix} = \mathcal{F}_u \left(\begin{bmatrix} D_{11} & C_1 & D_{12} \\ B_1 & A & B_2 \\ D_{21} & C_2 & D_{22} \end{bmatrix}, I_3\theta \right) \begin{bmatrix} x_K \\ u \end{bmatrix}$$

This transformation reduces the complexity of θ in $K_{LPV}(s,\theta)$, since θ is not repeated in $A_K(\theta(t)), B(\theta(t)), C(\theta(t))$ and $D(\theta(t))$ but occurs only once. With this realization, the related matrices are listed as below:

$$A = \begin{bmatrix} -4.5301 & -2612.1 & -131.06 & 193.44 & 98.995 & 47.589 & -41.269 & -8.4422 \\ 2640.2 & -37395 & 77398 & -116221 & -59215 & -27983 & 23891 & 5416.7 \\ -80.853 & 468.79 & -4075.4 & -9911.2 & -1816.2 & 2061.2 & -1600.5 & 1170.1 \\ -129.76 & 1293.5 & 5756.9 & -11144 & -4433.0 & 511.88 & -1975.4 & 2172.6 \\ 249.50 & -1779.2 & -1149.4 & 16932 & 6095.2 & 1643.2 & 3384.2 & -3267.4 \\ -328.35 & 2874.3 & 5640.6 & -28393 & -13090 & -829.59 & -4561.9 & 5234.0 \\ -1097.0 & 8725.4 & 7915.2 & -91020 & -36269 & 1798.3 & -16248 & 17843 \\ 278.66 & -2243.3 & -2280.2 & 25220.3 & 10344 & -619.34 & 4012.3 & -4840.8 \end{bmatrix}$$

$$B_1 = \begin{bmatrix} -0.09651 & 8.9632 & -10.206 \\ 55.657 & -4844.1 & 5680.0 \\ -1.5235 & 414.87 & 11.311 \\ -5.9535 & 2440.4 & -2100.0 \\ 8.8184 & -3867.4 & 3229.1 \\ -15.140 & 5572.3 & -4309.4 \\ -45.7728 & 17186 & -12987 \\ 12.308 & -4306.7 & 3159.4 \end{bmatrix}, \quad B_2 = \begin{bmatrix} -0.2321 \\ 148.51 \\ 41.497 \\ 58.073 \\ -85.43 \\ 132.77 \\ 467.92 \\ -130.58 \end{bmatrix}$$

$$
\begin{aligned}
C_1 &= \begin{bmatrix} -0.4918 & -286.57 & -14.425 & 21.660 & 11.036 & 5.2154 & -4.4528 & -1.0095 \\ 0.0076 & -0.0904 & 2.5651 & -2.8923 & -1.9579 & -0.9170 & 0.3092 & 0.6601 \\ 0.0070 & -0.1192 & 2.3009 & -2.6212 & -1.6963 & -0.7777 & 0.2801 & 0.5827 \end{bmatrix} \\
D_{11} &= \begin{bmatrix} 1.5864 \times 10^{-2} & 9.0284 \times 10^{-1} & -1.0586 \\ -1.7395 \times 10^{-3} & 2.4222 \times 10^{-1} & -4.7265 \times 10^{-1} \\ -1.4990 \times 10^{-3} & 5.7731 \times 10^{-1} & -7.4509 \times 10^{-1} \end{bmatrix}, \; D_{12} = \begin{bmatrix} -0.0276 \\ 0.0079 \\ 0.0069 \end{bmatrix} \\
C_2 &= \begin{bmatrix} 0.8770 & 511.01 & 25.722 & -38.625 & -19.679 & -9.3001 & 7.9401 & 1.8002 \end{bmatrix} \\
D_{21} &= \begin{bmatrix} -1.0393 & -1.6099 & 1.8877 \end{bmatrix}, \; D_{22} = 0.04935
\end{aligned}
$$

References

Assadian, F., 2002. A comparative study of optimal linear controllers for vibration suppression. Journal of the Franklin Institute 339 (3), 347–360.

Balas, M., 1978. Feedback control of flexible systems. IEEE Transactions on Automatic Control 23 (4), 673–679.

Bardou, O., Gardonio, P., Elliott, S., Pinnington, R., 1997. Active power minimization and power absorption in a plate with force and moment excitation. Journal of Sound and Vibration 208 (1), 111–151.

Bayon de Noyer, M., Hanagud, S., 1998. Single actuator and multi-mode acceleration feedback control. Journal of Intelligent Material Systems and Structures 9 (7), 522–533.

Baz, A., Poh, S., 1988. Performance of an active control system with piezoelectric actuators. Journal of Sound and Vibration 126 (2), 327–343.

Boyd, S., Barratt, C., 1992. Linear Controller Design: Limits of Performance. Prentice Hall Englewood Cliffs, NJ.

Boyd, S., Vandenberghe, L., 2004. Convex Optimization. Cambridge University Press.

Calafiore, G., Dabbene, F., Tempo, R., 2000. Randomized algorithms for probabilistic robustness with real and complex structured uncertainty. IEEE Transactions on Automatic Control 45, 2218–2235.

Carter, L., 1998. Linear parameter varying representations for nonlinear control design. Ph.D. thesis, The University of Texas at Austin, Texas, United States.

Chen, K., Huang, M., Fung, R., 2011. The comparisons of minimum-energy control of the mass-spring-damper system. In: 9th World Congress on Intelligent Control and Automation (WCICA). pp. 666–671.

Chettah, A., Ichchou, M., Bareille, O., Chedly, S., Onteniente, J., 2009. Dynamic mechanical properties and weight optimization of vibrated ground recycled rubber. Journal of Vibration and Control 15 (10), 1513–1539.

Darivandi, N., Morris, K., Khajepour, A., 2013. An algorithm for LQ optimal actuator location. Smart Materials and Structures 22 (3), 035001.

Dinh, M., 2005. Synthèse dépendant de paramètres par optimisation LMI de dimension finie: Application à la synthèse de correcteurs reréglables. Ph.D. thesis, Université de Caen/Basse-Normandie.

Dinh, M., Scorletti, G., Fromion, V., Magarotto, E., 2005. Parameter dependent H_∞ control by finite dimensional LMI optimization: application to trade-off dependent control. International Journal of Robust and Nonlinear Control 15 (9), 383–406.

Fialho, I., Balas, G., 2002. Road adaptive active suspension design using linear parameter-varying gain-scheduling. IEEE Transactions on Control Systems Technology 10 (1), 43–54.

Forrai, A., Hashimoto, S., Funato, H., Kamiyama, K., 2003. Robust active

vibration suppression control with constraint on the control signal: application to flexible structures. Earthquake engineering & structural dynamics 32 (11), 1655–1676.

Forrai, A., Tanoi, T., Hashimoto, S., Funato, H., Kamiyama, K., 2001. Robust controller design with hard constraints on the control signal. Electrical Engineering 83 (4), 179–186.

Gupta, V., Sharma, M., Thakur, N., 2010. Optimization criteria for optimal placement of piezoelectric sensors and actuators on a smart structure: a technical review. Journal of Intelligent Material Systems and Structures 21 (12), 1227–1243.

Gupta, V., Sharma, M., Thakur, N., 2012. Active structural vibration control: Robust to temperature variations. Mechanical Systems and Signal Processing 33, 167–180.

Hecker, S., 2006. Generation of low order LFT representations for robust control applications. Ph.D. thesis, Technical University Munich.

Hecker, S., Varga, A., J-F. Magni, 2005. Enhanced LFR-toolbox for Matlab. Aerospace Science and Technology 9 (2), 173–180.

Hegewald, T., Inman, D., 2001. Vibration suppression via smart structures across a temperature range. Journal of Intelligent Material Systems and Structures 12 (3), 191–203.

Ho, C., Lang, Z., Sapiński, B., Billings, S., 2013. Vibration isolation using nonlinear damping implemented by a feedback-controlled MR damper. Smart Materials and Structures 22 (10), 105010 (11 pages).

Huo, L., Song, G., Li, H., Grigoriadis, K., 2008. H_∞ robust control design of active structural vibration suppression using an active mass damper. Smart Materials and Structures 17, 015021.

Ichchou, M., Loukil, T., Bareille, O., Chamberland, G., Qiu, J., 2011. A reduced energy supply strategy in active vibration control. Smart Materials and Structures 20, 125008.

Iorga, L., Baruh, H., Ursu, I., 2009. H_∞ control with μ-analysis of a piezoelectric actuated plate. Journal of Vibration and Control 15 (8), 1143–1171.

J-F. Magni, 2006. User manual of the linear fractional representation toolbox. Technical report, ONERA, Systems, Control and Flight Dynamics Department.

Jemai, B., Ichchou, M., Jézéquel, L., 2002. Double panel partition (AVNC) by means of optimized piezoceramic structural boundary control. Journal of Vibration and Control 8 (5), 595–617.

Kim, S., Oh, J., 2013. A modal filter approach to non-collocated vibration control of structures. Journal of Sound and Vibration 332 (9), 2207–2221.

Kondoh, S., Yatomi, C., Inoue, K., 1990. The positioning of sensors and actuators in the vibration control of flexible systems. JSME International Journal. Ser. 3, Vibration, Control Engineering, Engineering for Industry 33 (2), 789–802.

Kumar, K., Narayanan, S., 2008. Active vibration control of beams with optimal placement of piezoelectric sensor/actuator pairs. Smart Materials and Structures 17 (5), 055008.

Kumar, R., 2012. Enhanced active constrained layer damping (ACLD) treatment using stand-off-layer: robust controllers design, experimental implementation and comparison. Journal of Vibration and Control 19 (3), 439–460.

Kumar, R., Singh, S., Chandrawat, H., 2006. Adaptive vibration control of smart structures: a comparative study. Smart Materials and Structures 15 (5), 1358.

Lee, H., Chen, S., Lee, A., 1996. Optimal control of vibration suppression in flexible systems via dislocated sensor/actuator positioning. Journal of the Franklin Institute 333 (5), 789–802.

Materazzi, A., Ubertini, F., 2012. Robust structural control with system constraints. Structural Control and Health Monitoring 19 (3), 472–490.

Meirovitch, L., 1986. Elements of Vibration Analysis, 2nd Edition. Sydney McGraw Hill.

Mohammadpour, J., Scherer, C. (Eds.), 2012. Control of Linear Parameter Varying Systems with Applications. Springer-Verlag, New York.

Moheimani, S., Fleming, A., 2006. Piezoelectric Transducers for Vibration Control and Damping. Springer Verlag, London.

Moreira, F., Arruda, J., Inman, D., 2001. Design of a reduced-order H_∞ controller for smart structure satellite applications. Philosophical Transactions: Mathematical, Physical and Engineering Sciences 359, 2251–2269.

N.J.M. van Dijk, Doppenberg, E., Faassen, R., van de Wouw, N., Oosterling, J., Nijmeijer, H., 2010. Automatic in-process chatter avoidance in the high-speed milling process. Journal of Dynamic Systems, Measurement, and Control 132 (3), 031006.

P. Van Phuoc, G. Nam Seo, P. Hoon Cheol, 2009. Vibration suppression of a flexible robot manipulator with a lightweight piezo-composite actuator. International Journal of Control, Automation and Systems 7 (2), 243–251.

Paijmans, B., Symens, W., Van Brussel, H., Swevers, J., 2006. A gain-scheduling-control technique for mechatronic systems with position-dependent dynamics. In: 2006 American Control Conference.

Qiu, Z., 2013. Experiments on vibration suppression for a piezoelectric flexible cantilever plate using nonlinear controllers. Journal of Vibration and Control.

Rasmussen, B., Alleyne, A., 2010. Gain scheduled control of an air conditioning system using the Youla parameterization. IEEE Transactions on Control Systems Technology 18 (5), 1216–1225.

Reinelt, W., 1999. H_∞ loop shaping for systems with hard bounds. In: Proc. of the Int Symp on Quantitative Feedback Theory and Robust Frequency Domain Methods. pp. 89–103.

Reinelt, W., 2000. Robust control of a Two-Mass-Spring system subject to its input constraints. In: 2000 American Control Conference. pp. 1817–1821.

Reinelt, W., 2001. Loop shaping of multivariable systems with hard constraints on the control signal. Electrical Engineering 83 (4), 169–177.

Rugh, W., Shamma, J., 2000. Research on gain scheduling. Automatica 36 (10), 1401–1425.

Saberi, A., A.A. Stoorvogel, Sannuti, P., 2000. Control of Linear Systems with Regulation and Input Constraints. Communications and Control Engineering. Springer Verlag, London.

Scherer, C., 2001. LPV control and full block multipliers. Automatica 37 (3), 361–375.

Scorletti, G., 1996. Some results about the stabilization and the L2-gain control of LFT systems. In: IEEE IMACS Multiconference on Computational Engineering in Systems Applications. pp. 1240–1245.

Scorletti, G., Fromion, V., 2008a. Automatique fréquentielle avancée. Ecole Centrale de Lyon, Master EEAP GSA, Université de Lyon 1, INSA de Lyon,http://cel.archives-ouvertes.fr/cel-0042384.

Scorletti, G., Fromion, V., 2008b. Synthesis tools for complex space systems, theory & concepts. Technical note, CNRS/INRA.

Scorletti, G., L. EI Ghaoui, 1998. Improved LMI conditions for gain scheduling and related control problems. International Journal of Robust and Nonlinear Control 8 (10), 845–877.

Sivrioglu, S., Nonami, K., Saigo, M., 2004. Low power consumption nonlinear control with H_∞ compensator for a zero-bias flywheel AMB system. Journal of Vibration and Control 10 (8), 1151–1166.

Skogestad, S., Postlethwaite, I., 2005. Multivariable Feedback Control-Analysis and Design. John Wiley and Sons.

Wang, Y., Inman, D., 2011. Comparison of control laws for vibration suppression based on energy consumption. Journal of Intelligent Material Systems and Structures 22 (8), 795–809.

Wang, Y., Inman, D., 2013a. Experimental validation for a multifunctional wing spar with sensing, harvesting, and gust alleviation capabilities. IEEE/ASME Transactions on Mechatronics 18 (4), 1289–1299.

Wang, Y., Inman, D., 2013b. Simultaneous energy harvesting and gust alleviation for a multifunctional composite wing spar using reduced energy control via piezoceramics. Journal of Composite Materials 47 (1), 125–146.

Wood, D., 1995. Control of parameter-dependent mechanical systems. Ph.D. thesis, Cambridge.

Yang, C., Sun, Y., 2002. Mixed H_2/H_∞ state-feedback design for microsatellite attitude control. Control Engineering Practice 10 (9), 951–970.

Zhang, K., Scorletti, G., Ichchou, M., Mieyeville, F., 2013. Phase and gain control policies for robust active vibration control of flexible structures. Smart Materials and Structures 22 (7), 075025 (15 pages).

Zhang, K., Scorletti, G., Ichchou, M., Mieyeville, F., 2014. Robust active vibration control of piezoelectric flexible structures using deterministic and probabilistic analysis. Journal of Intelligent Material Systems and Structures 25 (6), 665–679.

Zhang, X., Shao, C., Li, S., Xu, D., Erdman, A., 2001. Robust H_∞ vibration control for flexible linkage mechanism systems with piezoelectric sensors and actuators. Journal of Sound and Vibration 243 (1), 145–155.

Zhao, F., Fan, J., Mijanovic, S., 2013. PI auto-tuning and performance assessment in HVAC systems. In: 2013 American Control Conference. pp. 1783–1788.

Zhou, H., Zheng, X., Zhou, Y., 2006. Active vibration control of nonlinear giant magnetostrictive actuators. Smart Materials and Structures 15 (3), 792–798.

Zhou, K., Doyle, J., Glover, K., 1996. Robust and Optimal Control. Prentice, Hall Upper Saddle River, NJ.

Zorić, N., Simonović, A., Mitrović, Z., Stupar, N., 2013. Optimal vibration control of smart composite beams with optimal size and location of piezoelectric sensing and actuation. Journal of Intelligent Material Systems and Structures 24 (4), 499–526.